Genome-wide profiling of an enhancer-associated histone modification reveals the influence of asthma on the epigenome of the airway epithelium.

Authors:

Peter McErlean[1,2], Audrey Kelly[1,2], Jaideep Dhariwal[2,3], Max Kirtland[1,2], Julie Watson[1,2], Ismael Ranz[1,2], David J. Cousins[2,4], Roberto Solari[2,3], Michael R. Edwards[2,3], Sebastian L. Johnston[2,3] and Paul Lavender[1,2*] on behalf of the MRC-GSK Strategic Alliance Consortium.

Affiliations:

[1] Department of Respiratory Medicine and Allergy, King's College London, London, UK.

[2] MRC Asthma UK Centre in Allergic Mechanisms of Asthma, London, UK.

[3] Airway Disease Infection Section, National Heart and Lung Institute, Imperial College London, UK.

[4] NIHR Respiratory Biomedical Research Unit, Department of Infection, Immunity & Inflammation, Leicester Institute for Lung Health, University of Leicester, Leicester, UK

*Corresponding Author: paul.lavender@kcl.ac.uk

Author Contributions:

J.D. performed the clinical aspects of the study.

S.L.J. supervised clinical aspects of the study.

M.R.E performed clinical sample processing and culture.

P.M., A.K, J.W. performed ChIP Experiments.

P.M. and P.L. analyzed ChIP-Seq data.

P.M., M.K. performed dCas9 CRISPR work.

P.L., D.J.C., P.M, J.S., R.S., A.V.O., M.R.E and S.L.J conceived and designed the study.

Abstract

Asthma is a chronic airway disease driven by complex genetic-environmental interactions. The role of epigenetic modifications in bronchial epithelial cells (BECs) in asthma is poorly understood. We undertook genome-wide profiling of the enhancer-associated histone modification H3K27ac in BECs from people with asthma and healthy controls. We identified 49,903 regions exhibiting differential H3K27ac enrichment in asthma, clustered at genes associated with type-2-high asthma (*CLCA1*) and epithelial processes (EMT). Asthma dramatically influenced the BEC enhancer landscape and we identified asthma-associated Super-Enhancers encompassing genes encoding transcription factors (*TP63*) and enzymes regulating lipid metabolism (*NOX4*). We integrated published protein, epigenomic and transcriptomic datasets and identified epithelium-specific transcription factors associated with H3K27ac in asthma (*TP73*) and dynamic relationships between asthma-associated changes in H3K27ac, DNA methylation, genetic susceptibility and transcriptional profiles. Finally, we used a CRISPR-based approach to recapitulate the H3K27ac-asthma landscape *in vitro* and provide proof of principal that asthma-associated gene expression (*SERPINB2*) is driven in part by aberrant histone acetylation, validating the combination of genome-wide and epigenome-editing approaches in deciphering the molecular mechanisms underlying asthma pathogenesis.

Introduction:

Asthma is a chronic inflammatory disease of the airways affecting over 230 million people worldwide(1). Driven by complex genetic-environmental interactions, asthma's origins, triggers and clinical presentations are heterogeneous, posing challenges to understanding disease development, molecular components and the generation of more effective therapies(2).

The airway epithelium provides an initial physical barrier and biological responses to environmental insults. The airway epithelium of people with asthma is characterized by altered phenotypic and transcriptional characteristics including excessive mucus production, defects in antiviral responses and repair(3-5) and the predominance of signals associated with type 2 (T2) inflammation(6, 7). However, little is known about the molecular mechanisms that underpin the transcriptional profiles of airway epithelium in asthma.

The accessibility of areas within DNA contributing to transcription (transcription factor binding sites, regulatory elements/enhancers) is determined in part by epigenomic mechanisms including DNA methylation and histone modifications. Chromatin-immunoprecipitation coupled with high-through-put sequencing (ChIP-Seq) has revealed specific modifications on histone H3 are associated with various transcriptional states and genomic features. For example while occurring at transcriptional start sites (TSS's), H3 Lys4 dimethylation (H3K4me2) and H3 Lys27 acetylation (H3K27ac) are enriched predominately in intergenic (i.e. non-coding) regions and demarcate poised and active enhancers respectively(8).

Studies of epigenomic mechanisms have determined the epigenomes across a variety of cell types is altered in asthma(9-11). ChIP-Seq profiling of H3K4me2 in $CD4^+$ T cells from individuals with asthma has identified putative asthma-associated enhancers(10), supporting the use of genome-wide approaches to identify novel epigenomic mechanisms in asthma. However, while DNA methylation has been

broadly investigated(12-14), genome-wide investigations of histone modifications in the airway epithelium in asthma have yet to be undertaken.

Ranking ChIP-Seq signals revealed that regions of the genome exhibit increased enrichment of enhancer-associated histone modifications in a cell-type and disease-specific manner. These regions, termed 'Super-Enhancers' (SEs) differ from otherwise 'typical' enhancers by exhibiting sustained enrichment across several kilobases (kb), encompass 'master' transcription factors (TFs) important in cell-identity and are more likely to harbor disease-associated single nucleotide polymorphisms (SNPs)(15, 16). Super-Enhancers have been identified across numerous cell-types and diseases and are of potential interest for therapeutic intervention(17-19). However, airway epithelial cell and asthma-associated SEs have yet to be described.

Determining the functional consequences of epigenomic changes has been bolstered by the recent developments of the clustered, regularly interspaced, short palindromic repeats (CRISPR)-Cas9 system(20). By fusing catalytic domains of epigenome-modifying factors (e.g. DNA methyltransferases(21) and histone acetyltransferases(22)) to the catalytically-dead Cas9 (dCas9), site-specific epigenome editing can be achieved in a guide RNA (gRNA)-mediated manner and the consequence of epigenome alterations on gene transcription determined. Using dCas9-based editing, it is now possible to recapitulate disease-associated epigenomes *in vitro*, providing a means to accurately determine the contribution of aberrant epigenomic landscapes to disease-associated transcriptional profiles.

In the current study, we profiled H3K27ac via ChIP-Seq in bronchial epithelial cells (BECs) from people with asthma and healthy individuals. We undertook genome-wide analysis and identified regions of differential H3K27ac in asthma and by profiling an enhancer-associated histone modification, were able to identify airway epithelial and asthma-associated SEs. We additionally identified epithelial-specific TFs associated with H3K27ac in asthma and relationships between asthma-associated H3K27ac and DNA methylation, genetic susceptibility and transcriptional

profiles. Finally, we demonstrate by recapitulating the epigenomic landscape via a dCas9-based approach, that aberrant histone acetylation in asthma can drive asthma-associated gene expression.

Results:

Asthma influences H3K27ac enrichment in airway epithelial cells:

To investigate the influence of asthma on the epigenome of the airway epithelium, we profiled H3K27ac via ChIP-Seq in BECs from healthy controls (n=3) and adults with asthma (n=4, Table 1). Initial unbiased ChIP-Seq analysis revealed differences in H3K27ac between asthma and healthy volunteers (Figures 1A and S1A). We defined these differences more by comparing H3K27ac across consecutive, non-overlapping 1kb windows genome-wide (MEDIPS – see methods) and identified 49,903 differentially enriched regions in asthma (DERs, $P<0.05$, n=64 Adj $P<0.05$, Table 2).

Asthma DERs exhibited Gain and Loss in H3K27ac and were proximal to previously described asthma-associated genes (*CLCA1*, *POSTN*, *SERPINB2*)(6) as well as those not previously asthma-associated (Figure 1B-C). Only 1.4% of asthma DERs (n=663) overlapped with glucocorticoid receptor (GR) binding sites identified in dexamethasone-(DEX)-treated airway epithelial cells(23) (Figure S1C). Consistent with H3K37ac demarcating enhancers, asthma DERs localized at distal intergenic sites. However, loss of H3K27ac in asthma was greater around gene promoters, exons and untranslated regions (Figure S1B).

Although occurring genome-wide, asthma DERs clustered predominately around 3,800 genes (>n=3 DERs/gene, Figure S1D,E). Pathway analysis revealed DER-associated genes contributed to epithelial (e.g. gap junctions) and asthma-associated processes (e.g. leukotriene biosynthesis) with up to half of all genes within these pathways exhibiting differential H3K27ac in asthma (range 26.5%-57.1%, Figure 1E-G). Taken together, these data reveal that the airway epithelium in asthma is characterized by dynamic and distinct changes in the histone landscape.

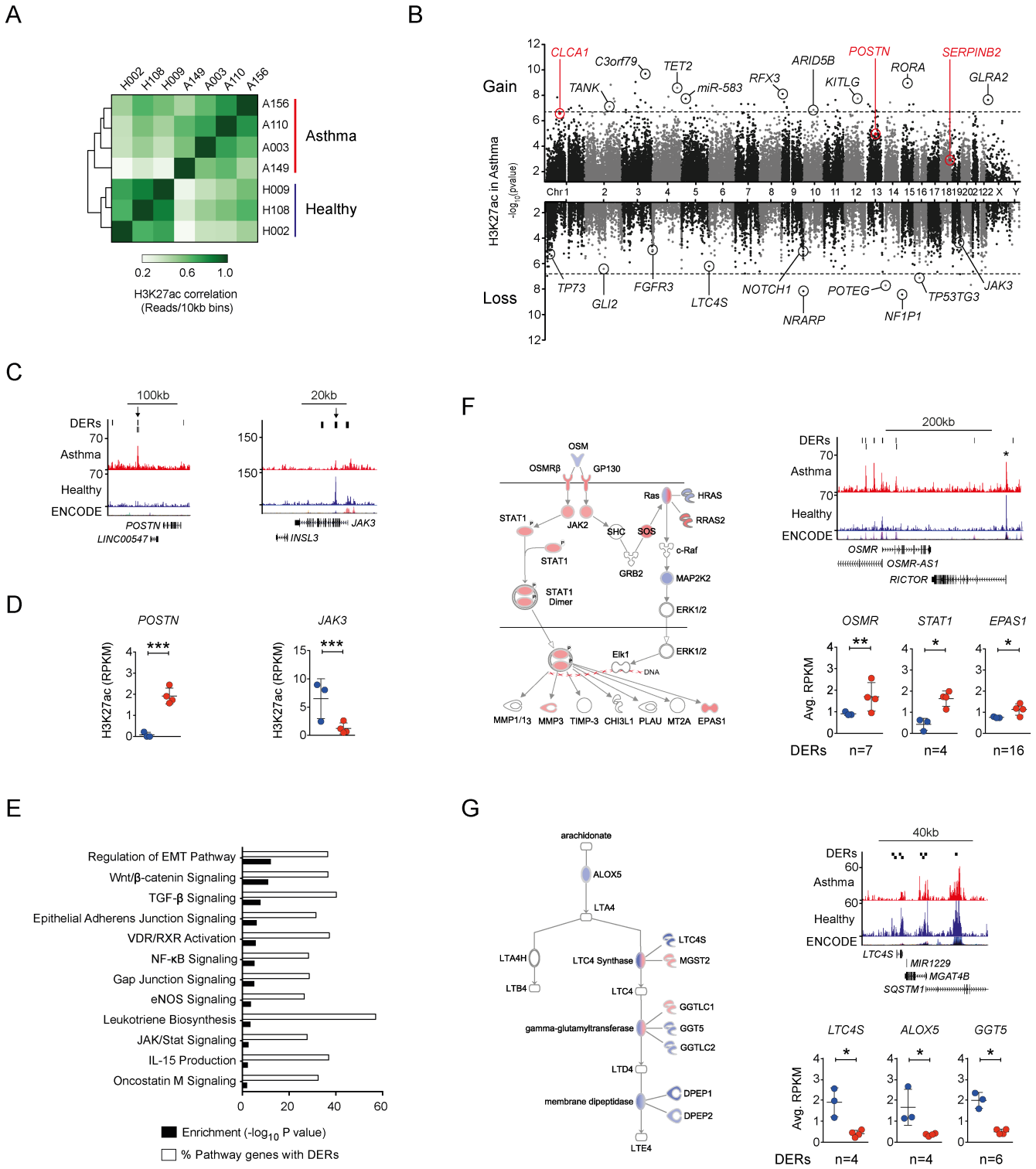
A
H002
H108
H009
A149
A003
A110
A156
Asthma
Healthy
0.2
0.6
1.0
H3K27ac correlation
(Reads/10kb bins)
B
Gain
Loss
H3K27ac in Asthma
-log10(pvalue)
CLCA1
C3orf79
TET2
TANK
miR-583
RFX3
ARID5B
KITLG
POSTN
RORA
SERPINB2
GLRA2
TP73
GLI2
FGFR3
LTC4S
NOTCH1
NRARP
POTEG
NF1P1
TP53TG3
JAK3
Chr 1 2 3 4 5 6 7 8 9 10 11 12 13 14 15 16 17 18 19 20 21 22 X Y
C
100kb
20kb
DERs
Asthma
Healthy
ENCODE
POSTN
LINC00547
JAK3
INSL3
D
POSTN
JAK3
H3K27ac (RPKM)
***
E
Regulation of EMT Pathway
Wnt/β-catenin Signaling
TGF-β Signaling
Epithelial Adherens Junction Signaling
VDR/RXR Activation
NF-κB Signaling
Gap Junction Signaling
eNOS Signaling
Leukotriene Biosynthesis
JAK/Stat Signaling
IL-15 Production
Oncostatin M Signaling
Enrichment (-log10 P value)
% Pathway genes with DERs
F
OSM
OSMRβ
GP130
STAT1
JAK2
SHC
SOS
Ras
HRAS
RRAS2
c-Raf
GRB2
MAP2K2
ERK1/2
STAT1 Dimer
Elk1
DNA
MMP1/13
MMP3
TIMP-3
CHI3L1
PLAU
MT2A
EPAS1
200kb
OSMR
OSMR-AS1
RICTOR
STAT1
Avg. RPKM
DERs n=7
n=4
n=16
G
arachidonate
ALOX5
LTA4
LTA4H
LTB4
LTC4 Synthase
LTC4S
MGST2
LTC4
gamma-glutamyltransferase
GGTLC1
GGT5
GGTLC2
LTD4
membrane dipeptidase
DPEP1
DPEP2
LTE4
40kb
MIR1229
MGAT4B
SQSTM1
ALOX5
GGT5
DERs n=4
n=4
n=6

Epithelial and asthma-associated Super-Enhancers are associated with enzymes involved in lipid metabolism:

Since we profiled an enhancer-associated histone modification, we sought to determine the enhancer landscape of the airway epithelium (H3K27ac enrichment >2kb from TSS's). We identified the regions exhibiting the greatest H3K27ac in merged datasets from healthy and asthma BECs (Peaks, MACS2 see methods) and ranked them based on ChIP-Seq signal (ROSE) to determine typical- and super-enhancer landscapes (SEs, Figure 2A). Given SEs can characterize cell-types and disease, we focused on the SEs specifically and observed a number of shared and unique SEs in this initial analysis. We subsequently identified and compared SEs from each volunteer revealing the presence of Common (airway cell-specific), Healthy and Asthma-associated SEs in BECs (Figures 2B-C).

Collectively, BEC-SEs were most closely related to SEs identified in mucosal cell-types and tissues (e.g. esophagus, lung and mammary epithelium, Figure S2A). However, BEC-SEs similarity to other SEs did not exceed 53.4%. We found BEC-SEs exhibited differential H3K27ac in asthma, with 95.5% containing DERs (range 1-44 DERs/SEs) covering on average 17.3% of the total SEs size (range 0.8%-90.2%; Table 3). While jointly typical- and super-enhancers overlapped 42.9% of asthma DERs (Figure S2B), plotting fold change of DERs across all enhancers identified dramatic changes in H3K27ac in SEs. Specifically, Asthma BECs exhibited marked decreases in H3K27ac in Common- and Healthy-SEs and increased H3K27ac in Asthma-SEs (Figures 2D and S2C).

Consistent with SEs encompassing 'master' TFs, we found between 10.8-15.7% of BEC-SE-associated genes encoded transcription regulators (Figure 2E), more so than typical enhancers (8.2%, Figure S2D). However, we additionally found BEC-SE-associated genes encoded enzymes (Table 3). Indeed, a higher proportion of asthma-SE-associated genes encoded enzymes than transcriptional regulators (18.15% vs. 11.9% respectively, Figure 2E). BEC-SE-associated enzymes were enriched in metabolic processes, particularly the conversion, synthesis and oxidation of lipids (Figure 2F,G). Further investigation revealed a number of lipid-associated enzymes

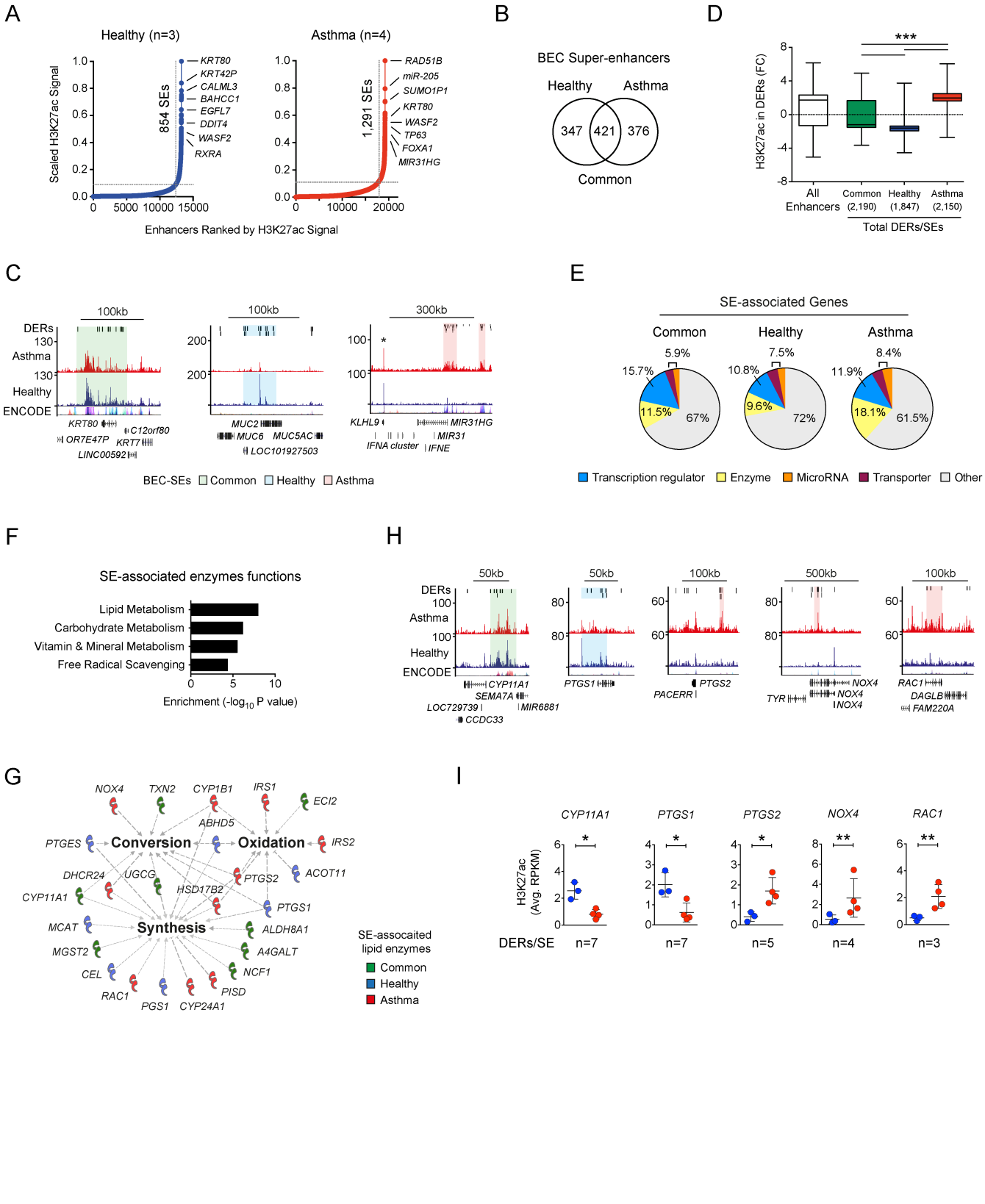
A
Healthy (n=3)
Asthma (n=4)
Scaled H3K27ac Signal
854 SEs
1,291 SEs
KRT80
KRT42P
CALML3
BAHCC1
EGFL7
DDIT4
WASF2
RXRA
RAD51B
miR-205
SUMO1P1
KRT80
WASF2
TP63
FOXA1
MIR31HG
Enhancers Ranked by H3K27ac Signal
B
BEC Super-enhancers
Healthy
Asthma
347
421
376
Common
D
H3K27ac in DERs (FC)
***
All Enhancers
Common (2,190)
Healthy (1,847)
Asthma (2,150)
Total DERs/SEs
C
100kb
100kb
300kb
DERs
Asthma
Healthy
ENCODE
KRT80
C12orf80
OR7E47P
KRT7
LINC00592
MUC2
MUC6
MUC5AC
LOC101927503
KLHL9
MIR31HG
MIR31
IFNA cluster
IFNE
BEC-SEs
Common
Healthy
Asthma
E
SE-associated Genes
Common
Healthy
Asthma
5.9%
15.7%
11.5%
67%
7.5%
10.8%
9.6%
72%
8.4%
11.9%
18.1%
61.5%
Transcription regulator
Enzyme
MicroRNA
Transporter
Other
F
SE-associated enzymes functions
Lipid Metabolism
Carbohydrate Metabolism
Vitamin & Mineral Metabolism
Free Radical Scavenging
Enrichment (-log10 P value)
H
50kb
50kb
100kb
500kb
100kb
DERs
Asthma
Healthy
ENCODE
CYP11A1
SEMA7A
LOC729739
MIR6881
CCDC33
PTGS1
PTGS2
PACERR
NOX4
TYR
RAC1
DAGLB
FAM220A
G
NOX4
TXN2
CYP1B1
IRS1
ECI2
ABHD5
PTGES
Conversion
Oxidation
IRS2
DHCR24
UGCG
PTGS2
ACOT11
CYP11A1
HSD17B2
PTGS1
MCAT
Synthesis
ALDH8A1
MGST2
A4GALT
CEL
NCF1
RAC1
PGS1
CYP24A1
PISD
SE-assocaited lipid enzymes
Common
Healthy
Asthma
I
CYP11A1
PTGS1
PTGS2
NOX4
RAC1
H3K27ac (Avg. RPKM)
DERs/SE
n=7
n=7
n=5
n=4
n=3

implicated in asthma pathogenesis to be encompassed by asthma-SEs (e.g. *PTGS2*, *NOX4*, *RAC1*; Figure 2H,I)(24, 25). Taken together, these data indicate that asthma has a dramatic influence on the location and enrichment of SEs in the respiratory epithelium.

Transcription factors associated with H3K27ac in asthma:

We next expanded on transcription regulators and identified enrichment of TF binding motifs in Asthma DERs and BEC-SEs. We focused on regions exhibiting the greatest H3K27ac overlapping DERs and BEC-SEs and identified motif enrichment in 28,420 peaks (mean size 240kb) representing 57.3% of DERs and 95.5% and BEC-SEs respectively. Enriched motifs were predominately from members of the FOX, HOX, Jun and Ets TF-families (Figure 3A).

To refine computational predictions and identify TFs associated with H3K27ac in the airway epithelium, we selected enriched TFs (P<1e-10) associated with either epithelial processes (Ingenuity), BEC-SEs or had protein expression in the respiratory epithelium(26) (n=253, Figures S3A,B and S4A, see methods). We found most TFs identified were expressed across many tissue types and in addition to epithelial biology (e.g. FOXA3) represented processes including circadian rhythm (e.g. CLOCK) and immediate early/inflammatory-response genes (e.g. JUN, Fos, Figure 3B). However, our approach identified those TFs expressed predominately in the respiratory epithelium (e.g. TP63).

Genes encoding TFs binding enriched motifs exhibited differential H3K27ac and healthy and asthma BECs displayed differences in H3K27ac enrichment profiles at TF binding sites identified in published ChIP-Seq studies (Figure S2C-E). We analyzed transcriptomic data derived from the largest study to date of asthma airway epithelium(27) and determined that 33.2% (n=84) enriched TFs also exhibited differential gene expression in asthma (Figure 3C and S4B).

We focused on Epithelium-dominant TFs with differential gene expression (Figure 3C,D) and found they were encompassed by BEC-SEs (Figure 3E and S3C) and

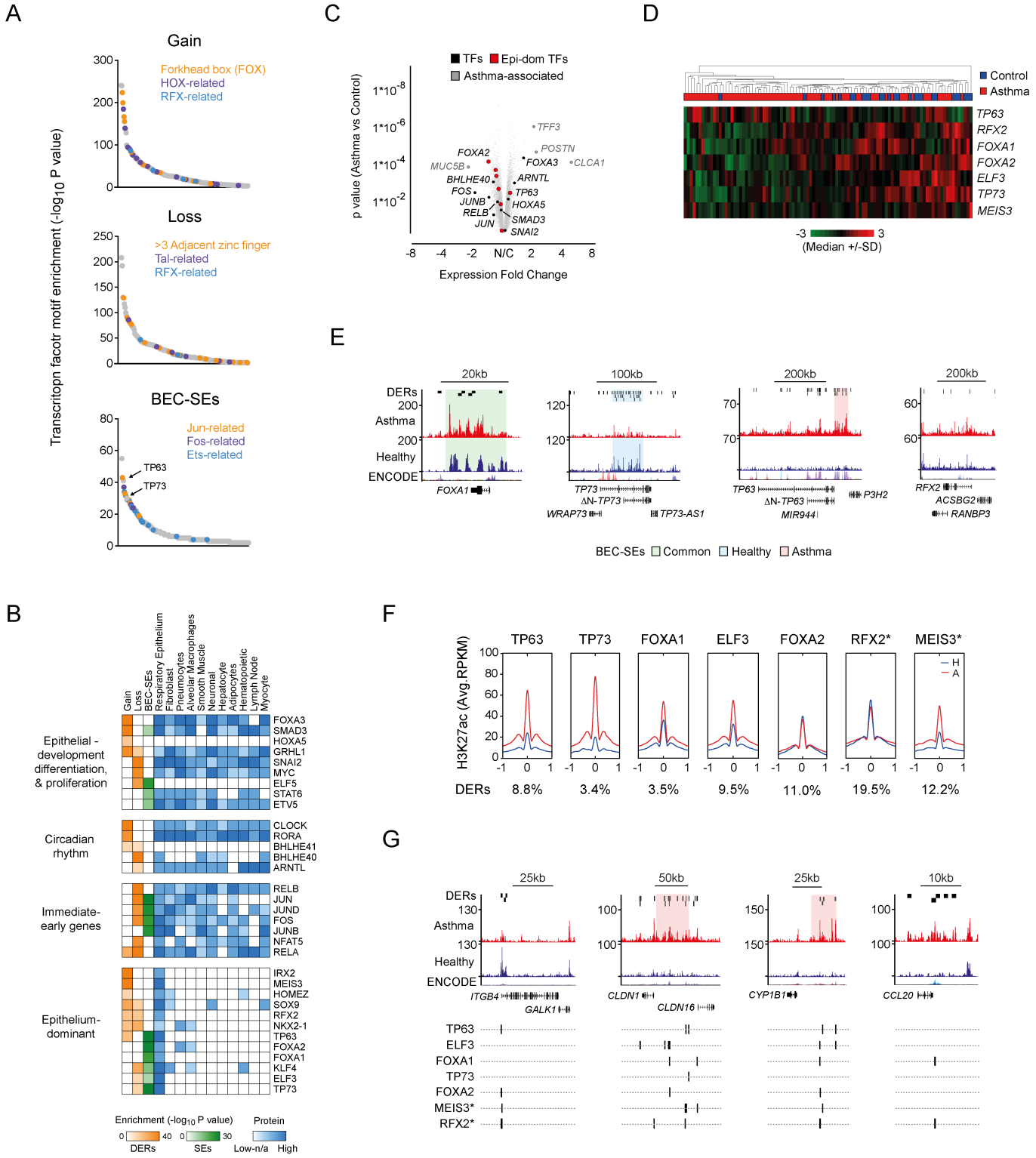
A
Gain
Forkhead box (FOX)
HOX-related
RFX-related
Loss
>3 Adjacent zinc finger
Tal-related
RFX-related
BEC-SEs
Jun-related
Fos-related
Ets-related
TP63
TP73
Transcritopn facotr motif enrichment (-log10 P value)
C
TFs
Epi-dom TFs
Asthma-associated
p value (Asthma vs Control)
Expression Fold Change
TFF3
POSTN
FOXA3
CLCA1
FOXA2
MUC5B
BHLHE40
ARNTL
FOS
TP63
JUNB
HOXA5
RELB
SMAD3
JUN
SNAI2
D
Control
Asthma
TP63
RFX2
FOXA1
FOXA2
ELF3
TP73
MEIS3
(Median +/-SD)
E
20kb
100kb
200kb
200kb
DERs
Asthma
Healthy
ENCODE
FOXA1
TP73
ΔN-TP73
WRAP73
TP73-AS1
TP63
ΔN-TP63
MIR944
P3H2
RFX2
ACSBG2
RANBP3
BEC-SEs
Common
Healthy
Asthma
B
Gain
Loss
BEC-SEs
Respiratory Epithelium
Fibroblast
Pneumocytes
Alveolar Macrophages
Smooth Muscle
Neuronal
Hepatocyte
Adipocytes
Hematopoietic
Lymph Node
Myocyte
Epithelial - development differentiation, & proliferation
FOXA3
SMAD3
HOXA5
GRHL1
SNAI2
MYC
ELF5
STAT6
ETV5
Circadian rhythm
CLOCK
RORA
BHLHE41
BHLHE40
ARNTL
Immediate-early genes
RELB
JUN
JUND
FOS
JUNB
NFAT5
RELA
Epithelium-dominant
IRX2
MEIS3
HOMEZ
SOX9
RFX2
NKX2-1
TP63
FOXA2
FOXA1
KLF4
ELF3
TP73
Enrichment (-log10 P value)
DERs
SEs
Protein
Low-n/a
High
F
TP63
TP73
FOXA1
ELF3
FOXA2
RFX2*
MEIS3*
H3K27ac (Avg.RPKM)
H
A
DERs
8.8%
3.4%
3.5%
9.5%
11.0%
19.5%
12.2%
G
25kb
50kb
25kb
10kb
DERs
Asthma
Healthy
ENCODE
ITGB4
GALK1
CLDN1
CLDN16
CYP1B1
CCL20
TP63
ELF3
FOXA1
TP73
FOXA2
MEIS3*
RFX2*

included those previously implicated in mouse models of allergic inflammation (*FOXA2*, *ELF3*)(28-30), asthma, nasal polyposis and mucociliary development (*TP63*, *TP73*, *RFX2*)(31-34). Profiling revealed Asthma BECs exhibited more H3K27ac at epithelial-TF ChIP-Seq sites, encompassing up to 9.5% of asthma DERs (Figure 3F). Similar profiles and DER coverage was observed at predicted sites for those epithelial TFs for which no ChIP-Seq data is yet available (Figure S3E). Finally, we found bona-fide and predicted Epithelium-dominant TF binding sites co-localized in DERs populating genes associated with epithelial integrity (e.g. *ITGB4*, *CLDN1*), metabolism (e.g. *CYP1B1*) and inflammatory cell recruitment (e.g. *CCL20*, Figure 3G). These findings suggest that asthma-associated changes in the histone landscape are likely mediated by a combination of airway cell-specific and otherwise ubiquitously expressed TFs.

Asthma-associated changes in H3K27ac and DNA methylation are related but limited.

To investigate how changes in H3K27ac related to other epigenomic mechanisms in asthma, we investigated the relationship between asthma DERs, BEC-SEs and DNA methylation identified in the largest study to date of methylation of airway epithelium in asthma(13). We found asthma DERs contained differentially methylated CpGs (Figure 4A) with most overlap occurring within CpG islands (CGI's, Figure 4B) and a weak but significant relationship between asthma-associated changes in H3K27ac and CpG methylation (Figure 4C). However, this relationship accounted for only 7.0% (n=2,875) and 4.7% (n=2,394) of differentially methylated CpGs and asthma DERs respectively.

We focused on differentially methylated CpGs residing within CGI's and identified a striking relationship with loss of H3K27ac in asthma (Figure 4C). Further investigation revealed Loss DERs contained increased CpG content, reflecting a high proportion overlapping CGI's (Figure 4D). However, despite this relationship, we observed discordance between asthma-associated CpG methylation and H3K27ac even across CGI's of the same gene locus (Figure 4E).

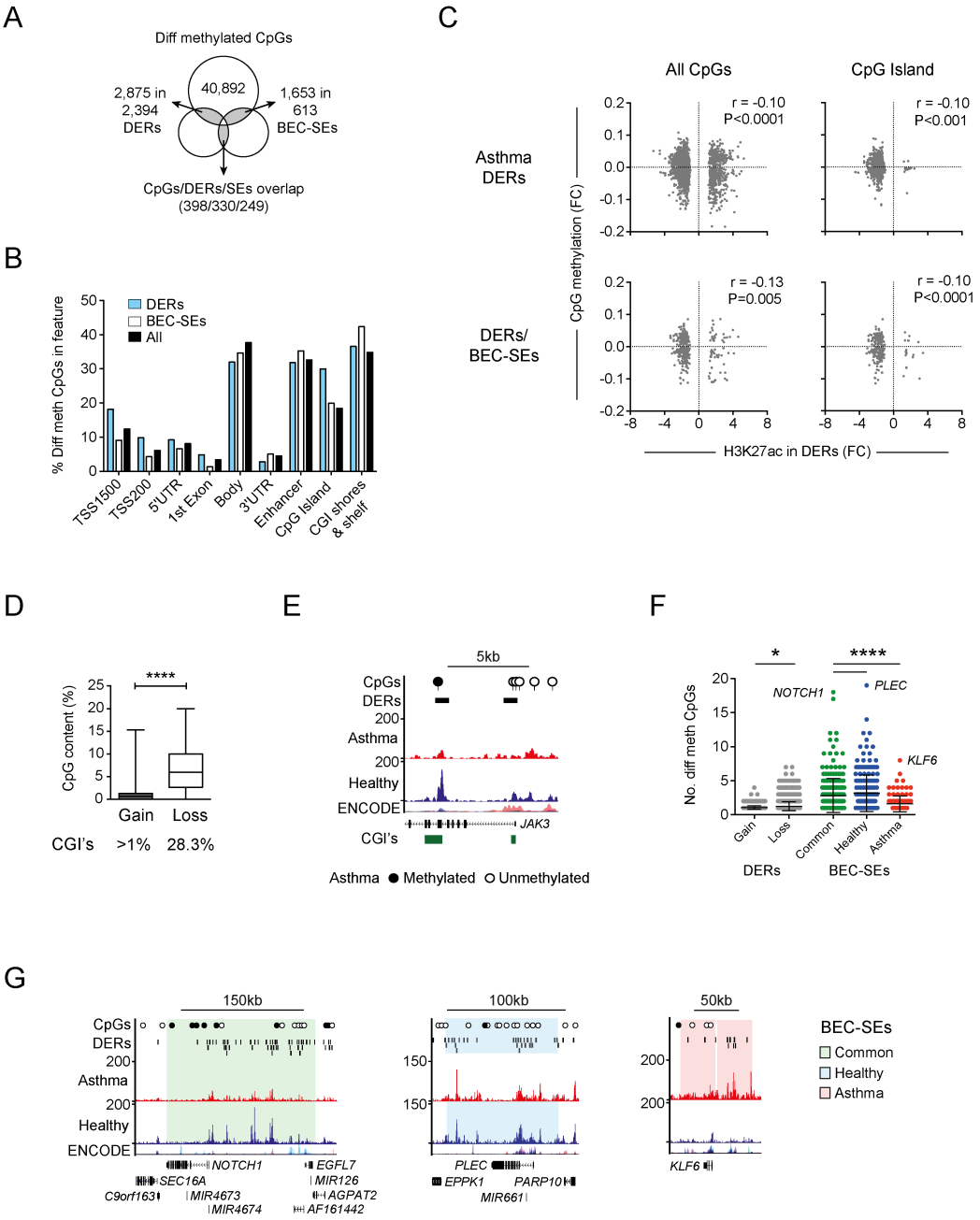
A
Diff methylated CpGs
40,892
2,875 in 2,394 DERs
1,653 in 613 BEC-SEs
CpGs/DERs/SEs overlap (398/330/249)
B
% Diff meth CpGs in feature
DERs
BEC-SEs
All
TSS1500
TSS200
5'UTR
1st Exon
Body
3'UTR
Enhancer
CpG Island
CGI shores & shelf
C
All CpGs
CpG Island
Asthma DERs
DERs/ BEC-SEs
CpG methylation (FC)
r = -0.10
P<0.0001
r = -0.10
P<0.001
r = -0.13
P=0.005
r = -0.10
P<0.0001
H3K27ac in DERs (FC)
D
CpG content (%)
****
Gain
Loss
CGI's
>1%
28.3%
E
5kb
CpGs
DERs
Asthma
Healthy
ENCODE
JAK3
CGI's
Asthma ● Methylated ○ Unmethylated
F
No. diff meth CpGs
*
****
NOTCH1
PLEC
KLF6
Gain
Loss
Common
Healthy
Asthma
DERs
BEC-SEs
G
150kb
100kb
50kb
CpGs
DERs
Asthma
Healthy
ENCODE
NOTCH1
EGFL7
SEC16A
MIR126
C9orf163
MIR4673
AGPAT2
MIR4674
AF161442
PLEC
EPPK1
PARP10
MIR661
KLF6
BEC-SEs
Common
Healthy
Asthma

Within BEC-SEs, weak but significant relationships were also evident between changes in H3K27ac, all differentially methylated CpGs and those residing within CGI's (Figure 4C). A similar relationship was identified for those CpGs annotated within predicted enhancers (Figure S5A). Interestingly, while accounting for only 4.0% (n=1,653) of asthma-associated CpG methylation, we found 53.5% (n=613) of BEC-SEs contained differentially methylated CpGs, with most populating Common- and Healthy-SEs (Figure 4F). However we again observed dynamic changes in asthma-associated CpG methylation across BEC-SEs (Figure 4G). Finally, genes encoding DNA methylation-associated enzymes exhibit marked changes in H3K27ac and expression levels in asthma (e.g. *TET2*, *MBD2*, Figure S4C and S5B,C). These data suggest that while evident, concurrent alterations in epigenomic mechanisms may only account for a fraction of asthma-associated changes in the histone landscape.

Interactions between Asthma-associated H3K27ac and SNPs are mediated via 3D chromatin architecture.

Since previous studies have identified enrichment of disease-associated SNPs in enhancers(10), we looked at the relationship between change in H3K27ac and asthma susceptibility. We found asthma SNPs overlapped DERs at key asthma-associated genes including *IL-6*, *TSLP* and *IL1RL1* (also known as the IL33 receptor ST2, Figure 5A,B and Table 4). Remarkably, we observed that the H3K27ac at overlapping SNPs was dynamic, even across SNPs within the same haplotype block (e.g. rs10062929 - gain and rs1370964 - loss, Figure 5B). However, while we did not observe a statistical enrichment of asthma SNPs in DERs or BEC-SEs (*P*=0.97 and *P*=0.31 respectively, *Chi* square Vs all SNPs within DERs/SEs, data not shown), we found over 70% of Asthma SNPs had a DER or enhancer within 200kb (Figures 5C and S2E).

Given most SNPs reside within non-coding regions and may influence long-range chromosomal interactions(13, 35), we investigated the relationship between SNPs, DERs and 3D chromatin architecture. Since no interaction dataset is available for primary respiratory epithelial cells, we utilized Hi-C data from whole lung tissue(36) and focused on the asthma susceptibility locus 17q21. While previous reports have

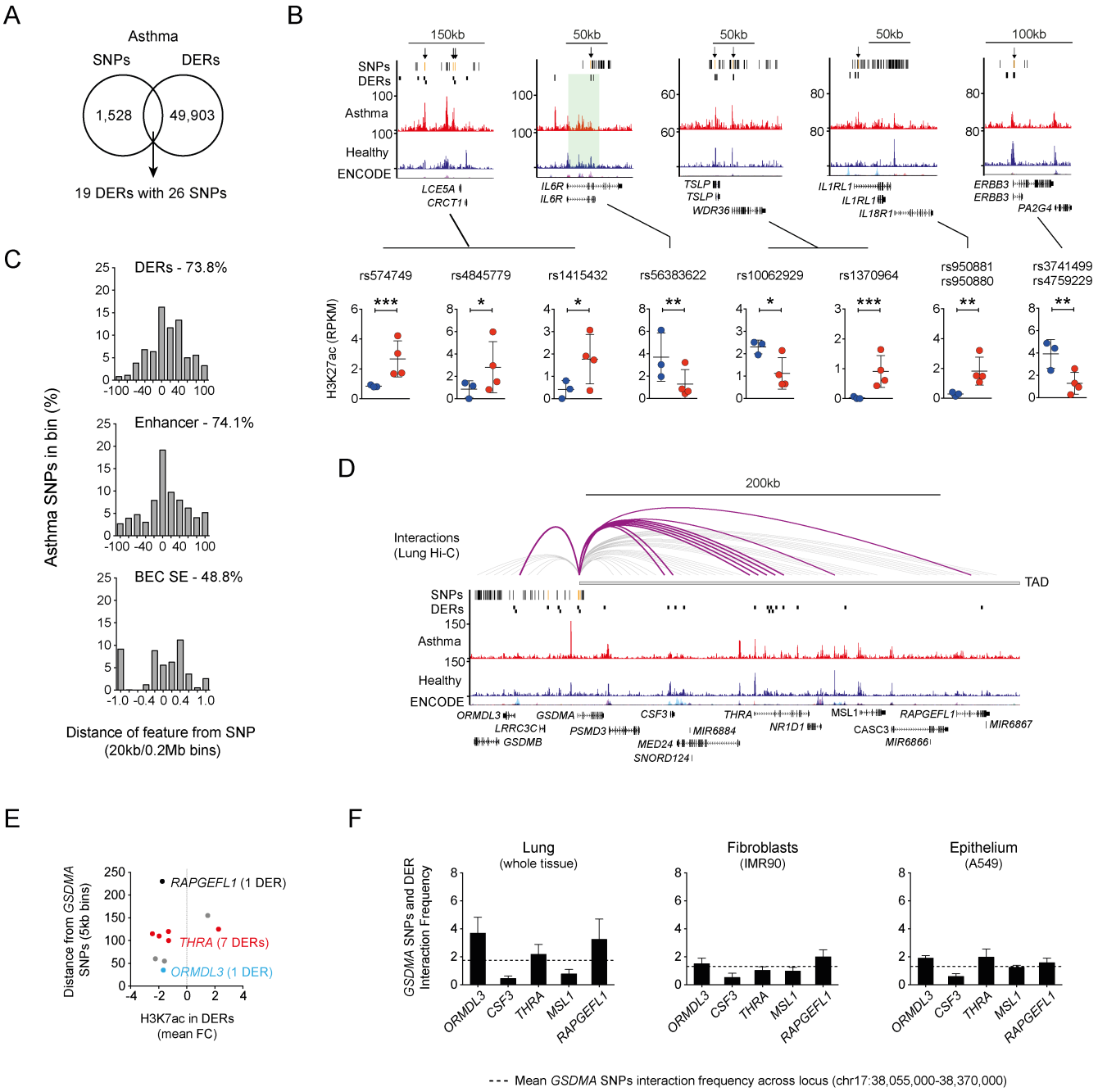
A
Asthma
SNPs
DERs
1,528
49,903
19 DERs with 26 SNPs
B
150kb
50kb
50kb
50kb
100kb
SNPs
DERs
Asthma
Healthy
ENCODE
LCE5A
CRCT1
IL6R
IL6R
TSLP
TSLP
WDR36
IL1RL1
IL1RL1
IL18R1
ERBB3
ERBB3
PA2G4
rs574749
rs4845779
rs1415432
rs56383622
rs10062929
rs1370964
rs950881
rs950880
rs3741499
rs4759229
H3K27ac (RPKM)
C
DERs - 73.8%
Enhancer - 74.1%
BEC SE - 48.8%
Asthma SNPs in bin (%)
Distance of feature from SNP
(20kb/0.2Mb bins)
D
200kb
Interactions
(Lung Hi-C)
TAD
SNPs
DERs
Asthma
Healthy
ENCODE
ORMDL3
GSDMA
CSF3
THRA
MSL1
RAPGEFL1
LRRC3C
PSMD3
MIR6884
NR1D1
CASC3
MIR6867
GSDMB
MED24
MIR6866
SNORD124
E
Distance from GSDMA
SNPs (5kb bins)
RAPGEFL1 (1 DER)
THRA (7 DERs)
ORMDL3 (1 DER)
H3K7ac in DERs
(mean FC)
F
Lung
(whole tissue)
Fibroblasts
(IMR90)
Epithelium
(A549)
GSDMA SNPs and DER
Interaction Frequency
ORMDL3
CSF3
THRA
MSL1
RAPGEFL1
--- Mean GSDMA SNPs interaction frequency across locus (chr17:38,055,000-38,370,000)

described interactions between SNPs at ORDML3 and regions upstream including *IKZF3* (13, 35), we found SNPs overlapping DERs at *GSDMA* (Table S4) occur at the boundary of a topologically associated domain (TAD) and interact with other DER-containing regions downstream (Figures 5D). Interactions spanned ~200kb and were predominately with DERs losing H3K27ac in asthma (Figures 5E). *GSDMA* SNPs/DERs interactions were strongest with DER-containing regions encompassing *ORMDL3*, *THRA* and *RAPGEFL1* in lung tissue, but not in cell types representing other components of the respiratory system (e.g. fibroblasts, epithelium, Figure 5F). Taken together, these data suggest that 3D chromatin architecture dictates interactions between disease-associated polymorphisms and epigenomic changes in asthma.

Alterations to H3K27ac are related to asthma-associated transcriptional profiles: Since histone acetylation is associated with transcriptional activation, we expanded on our transcriptomic analysis (Figure 3C) and investigated the relationship between H3K27ac and all asthma-associated gene expression(27). We determined that H3K27ac was likely to influence 34.0% of differential gene expression in asthma (n=1,592 genes, Table 5) and gain and loss of H3K27ac was associated with up and down regulation in expression respectively (Figure 6A). However, we observed discordance in the relationship between H3K27ac and expression across a number of genes (Figure 6B-D and Table 5).

Given most asthma DERs resided within intergenic regions (Figure S1B), we investigated if similar to SNPs; DERs may influence gene expression via long-range interactions. We again utilized Lung Hi-C data and focused on the relationship between DERs and 3D architecture across the locus of the Th2-high signature gene *CLCA1*(37) (Figure 6E). Surprisingly, there was minimal H3K27ac enrichment in either healthy or asthma BECs across *CLCA1* itself. However, we observed interactions between *CLCA1* and asthma DERs spanning ~200kb, including those residing within an asthma-SE encompassing *CLCA2* (Figure 6E,G). Interactions with *CLCA2* and *CLCA3P* were strongest in lung tissue and epithelium respectively (Figure 6F). Taken together, these data reveal complexity between the histone landscape and gene

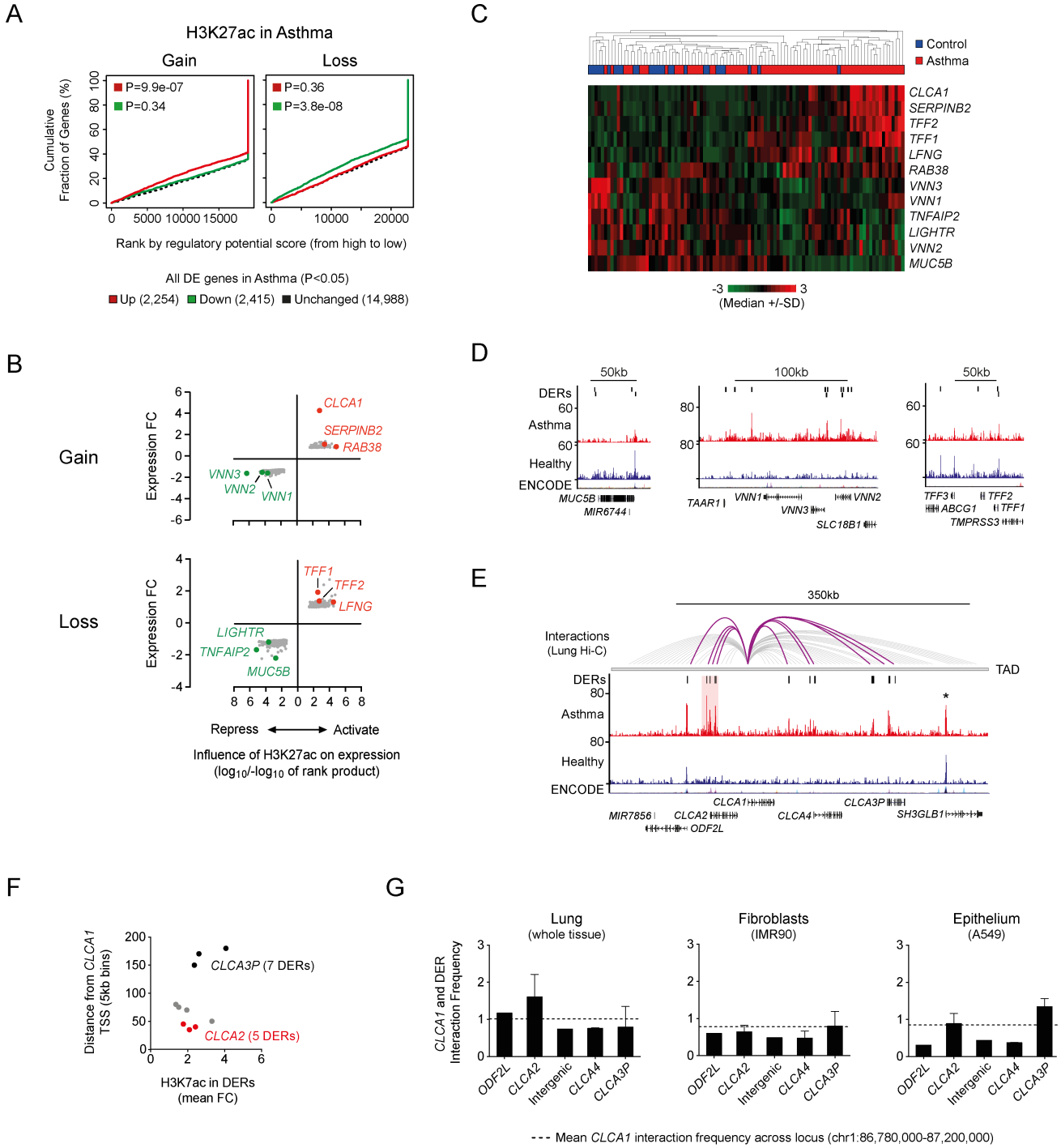
A
H3K27ac in Asthma
Gain
Loss
P=9.9e-07
P=0.34
P=0.36
P=3.8e-08
Cumulative Fraction of Genes (%)
Rank by regulatory potential score (from high to low)
All DE genes in Asthma (P<0.05)
Up (2,254)
Down (2,415)
Unchanged (14,988)
B
Gain
Loss
Expression FC
CLCA1
SERPINB2
RAB38
VNN3
VNN2
VNN1
TFF1
TFF2
LFNG
LIGHTR
TNFAIP2
MUC5B
Repress
Activate
Influence of H3K27ac on expression
(log10/-log10 of rank product)
C
Control
Asthma
CLCA1
SERPINB2
TFF2
TFF1
LFNG
RAB38
VNN3
VNN1
TNFAIP2
LIGHTR
VNN2
MUC5B
-3
3
(Median +/-SD)
D
50kb
100kb
50kb
DERs
Asthma
Healthy
ENCODE
MUC5B
MIR6744
TAAR1
VNN1
VNN2
VNN3
SLC18B1
TFF3
TFF2
ABCG1
TFF1
TMPRSS3
E
350kb
Interactions
(Lung Hi-C)
TAD
DERs
Asthma
Healthy
ENCODE
CLCA1
CLCA3P
MIR7856
CLCA2
CLCA4
SH3GLB1
ODF2L
F
Distance from CLCA1 TSS (5kb bins)
CLCA3P (7 DERs)
CLCA2 (5 DERs)
H3K7ac in DERs
(mean FC)
G
Lung
(whole tissue)
Fibroblasts
(IMR90)
Epithelium
(A549)
CLCA1 and DER Interaction Frequency
ODF2L
CLCA2
Intergenic
CLCA4
CLCA3P
--- Mean CLCA1 interaction frequency across locus (chr1:86,780,000-87,200,000)

transcription and further implicates 3D architecture in asthma-associated gene expression.

Transcriptional consequences of H3K27ac in asthma:

Finally, to begin to clarify the relationship between H3K27ac and gene expression in asthma, we employed a dCas9-based editing approach to recapitulate the epigenome we observed in asthma BECs, in human embryonic kidney (HEK293T) cells. Using dCas9 fused with the catalytic core of histone acetyltransferase P300 (dCas9-P300-Core)(22), we targeted acetylation via gRNAs to DERs gaining H3K27ac at genes representing Th2-high asthma (*SERPINB2*), antiviral responses (*TLR3*) and a mediator of inflammatory cell recruitment (*TSLP*, Figure 7A-B). We found gene expression could be selectively induced using DER-specific gRNAs only in the presence of the active form of dCas9-P300-Core (Figures 7C). Additionally, we found these acetylation-dependent transcriptional effects could be mediated using either pooled or single DER-specific gRNAs (Figure S6A,B). These data indicate acetylation of regions exhibiting differential H3K27ac in asthma can drive asthma-associated gene expression.

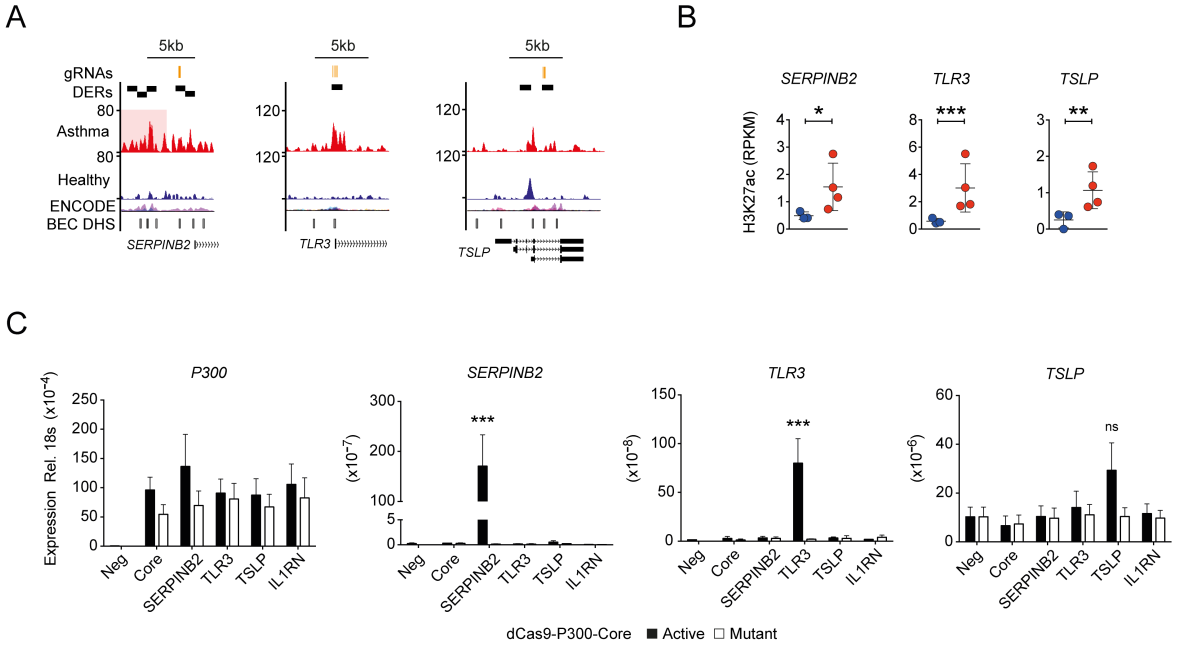
A
5kb
gRNAs
DERs
Asthma
Healthy
ENCODE
BEC DHS
SERPINB2
TLR3
TSLP
B
SERPINB2
TLR3
TSLP
H3K27ac (RPKM)
C
P300
Expression Rel. 18s (x10⁻⁴)
Neg
Core
SERPINB2
TLR3
TSLP
IL1RN
ns
dCas9-P300-Core
Active
Mutant

Discussion:

Consistent with studies of other epigenomic mechanisms, we found that asthma influences the histone landscape in the airway epithelium. We investigated H3K27ac in order to survey the effects of asthma across both TSS's and intergenic/enhancer regions. We identified close to 50K regions covering 1.6% of the genome exhibiting differential H3K27ac in asthma (Figure 1B and Tables 1). DERs occurred at regions exhibiting H3K27ac enrichment in other cells types (Figure S1B and ENCODE data tracks) and clustered predominately around asthma- and epithelial-associated genes (Figure 1E). Although our study contained small sample numbers, our data adds to growing evidence that chronic inflammatory airway disease is characterized by distinct changes to the epigenome.

By profiling an enhancer-associated histone modification we were able to identify for the first time, to our knowledge, airway epithelial cell- and asthma-associated SEs (Figure 2). Our data supports findings that chronic inflammatory diseases are characterized by distinct SE landscapes(19). We found that asthma-SEs encompassed asthma-associated transcription factors (e.g. *TP63*)(31), non-coding RNAs regulating cell function following viral infection (e.g. *miR-31*)(38) and enzymes important in lipid metabolism (e.g. *NOX4*, *RAC1*, Table 3)(25).

While well established that SEs encompass 'master' TFs(16), the association of SEs with enzymes is not readily described. Lipid mediators are key components of the inflammatory response and targets of current (e.g. montelukast) and novel asthma therapies (e.g. fevipiprant)(39). Perturbations in the epigenome surrounding enzymes responsible for mediator synthesis may therefore have dramatic effects on the severity and duration of inflammation and subsequent disease management.

The identification of asthma-associated SEs raises the possibility of targeting the epigenome as a therapeutic option in asthma. Peeters *et. al*(19) saw a reduction in pro-inflammatory gene expression in $CD4^+$ T cells when targeting arthritis-associated SEs with JQ1, an inhibitor of the epigenome 'reader' bromodomain and extra

terminal proteins (BET). A similar reduction in antiviral gene expression following JQ1 treatment was observed in PBMCs and macrophages from COPD patients by Malhotra *et. al* (40). However, while providing anti-inflammatory capacity, broad targeting of the epigenome with BET or other inhibitors warrants further investigation, considering we identified many regions losing H3K27ac in asthma BECs (Figure S1D).

The striking loss of H3K27ac at Common- and Healthy-SEs (Figure 2D) suggests that the otherwise 'normal' function of epithelial cells is broadly affected in asthma. These findings provide further insights into non-inflammatory aspects of the asthmatic airways namely defects in repair and differentiation(4). Indeed, TP73 has a key role in mucociliary development(34) and exhibited a dramatic loss of H3K27ac in asthma BECs (Figure 3B). Our findings suggest defects in the asthmatic epithelium are epigenomic in origin and may explain why these characteristics are maintained *ex vivo*.

We sought to identify the molecular components associated with changes in H3K27ac and augmented TF motif enrichment with pathway analyses, protein expression and transcriptomic data (Figure 3). We found the majority of TF's binding enriched motifs in DERs and BEC-SEs were expressed across many tissue types (Figure 3A) and genes encoding TFs exhibited differential H3K27ac in asthma (Figure S2D). By altering the epigenomic landscape and subsequent gene expression profiles, asthma may influence TF-complex binding profiles, chromatin architecture and key processes of the airway epithelium.

In keeping with these data, TFs with pioneer or chromatin remodeling capacity (e.g. FOXA-family members and AP1) are differentially expressed in asthmatic bronchial epithelial cells(27, 41) and FOX and RFX-family members have been shown to interact and drive cilia-associated gene expression in the airway epithelium(42). In addition, we found TFs associated with circadian rhythm to be represented in our dataset (Figure 3A). Studies implicate the dysregulation of the circadian clock as a characteristic of chronic inflammatory disease such as arthritis and asthma(43, 44)

and components of the circadian clock show altered expression following allergen challenge of nasal epithelial cells(45). Our findings suggest that this dysregulation may also mediate changes in the epigenome, considering CLOCK has histone acetyltransferase activity and other epigenetic modifying enzymes exhibit binding in a circadian manner. Therefore, further genome-wide profiling of epithelial-dominant and other TFs is required to determine the factors initiating and exploiting changes we observed in the histone landscape of the asthma airway epithelium.

While we did not identify a statistical enrichment of Asthma SNPs in DERs or BEC-SEs, we identified a long-range interaction between SNPs and DERs across the 17q21 locus (Figure 5D-F). Interestingly these interactions involved *THRA*, which overlaps the antisense transcribed *NR1D1* (also known as Rev-erbα) a key regulator of circadian rhythm and lipid metabolism (Figure 5D). These observations add to growing evidence that SNPs mediate their effects through long-range interactions. Schmiedel *et. al*(35) reported that asthma-risk alleles perturb CTCF binding and long-range interactions involving the promoter of *ORMDL3* in $CD4^+$ cells. Given GSDMA SNPs/DERs overlap at a TAD boundary (Figure 5D), it is possible that asthma risk alleles may also influence long-range interactions in airway epithelial cells. Furthermore, changes in DNA methylation at asthma SNPs are also implicated with long-range interactions across 17q21(13). Future studies should therefore seek to integrate genetic, epigenomic and 3D architecture data to accurately determine quantitative trait loci in key cell types of asthma(46).

To gain an overall understanding of the influence of asthma on the epigenome and gene transcription, we integrated our data with those derived from the largest studies to date of DNA methylation and gene expression in the airway epithelium of people with asthma. However, while providing important insights into the relationships between epigenomics and transcriptomics, our data integration approach has equally identified the complexity of these relationships.

Based on the 450K DNA methylation array platform, Nicodemus-Johnson *et. al*(13) reported over 40K differentially methylated CpGs in bronchial brushings of asthmatic

individuals compared to healthy controls. Although numerous, the degree of methylation change exhibited by asthmatics at individual CpGs did not exceed 20% (mean -0.09%, median -0.01%). Regardless, we investigated the relationship between H3K27ac and CpG methylation and found a weak, but statistically significant correlation (Figure 4A). However, this relationship accounted for less than 10% and 5% of differentially methylated CpGs and of asthma DERs respectively (Figure 4).

These data likely reflect the CpGs assayed on the 450K array occur predominately in TSS-associated CGI's rather than intergenic regions. The occurrence of Loss DERs at gene promoters (Figure S1B) and the relationship between loss of H3K27ac and differentially methylated CpGs in CGI's would support this speculation (Figure 4D). Furthermore, while the predominance of differentially methylated CpGs in BEC-SEs encompassing epithelial-associated genes is noteworthy (e.g. *NOTCH1*, *PLEC,* Figure F-G), it is hard to determine if BEC-SEs contain more differentially methylated CpGs than would occur by chance. Deciphering relationships between epigenomic marks in future studies should therefore employ genome-wide approaches (e.g. whole genome bisulfite-seq, ChIP-Seq).

Traditionally, histone acetylation is a hallmark of transcriptional activation and we found that the gain and loss of H3K27ac was associated with concurrent changes in gene expression in asthma. However, we found discordance in this association across a number of genes (Figure 6B). While we surveyed only one of the many histone modifications and factors that contribute to gene transcription, Cinghu *et.* al(47) has recently found that intragenic enhancers attenuate gene expression during transcriptional elongation. Furthermore, long-range interactions may also influence the relationship between H3K27ac and gene expression (Figure 6D). Taken together these data raise the possibility that in addition to being associated with 'active enhancers', H3K27ac broader role as a marker of regulatory elements may include transcriptional repressors dictated by polymerase/TF-occupancy and 3D architecture.

To validate our ChIP-Seq analysis and identify a functional consequence of H3K27ac in asthma, we employed a CRISPR-Cas9-based approach to recapitulate the epigenome of asthma BECs in human embryonic kidney (HEK293T) cells *in vitro*. We targeted acetylation to asthma DERs at *SERPINB2*, *TLR3* and *TSLP* and found that gene expression could be induced in an acetylation and DER-specific gRNA manner, providing evidence that asthma-associated transcriptional profiles are driven in part by aberrant acetylation (Figure 7C). However, we found targeting of DERs within an asthma-SEs did not result in induction of gene expression (Figure S6C). These data suggest that some enhancers may require additional stimuli to be functional (e.g. by altering 3D architecture bringing enhancers/TF complexes to gene promoters). The failure to induce *IFNB* gene expression after targeting acetylation alone to an upstream virus-inducible enhancer(48) would support these speculations (Figure S6D). Regardless, the ability to manipulate the epigenome in a site-specific manner provides a tremendous tool to clarify the functional consequences of disease-associated changes in the epigenome.

It remains to be determined what the trigger(s) mediating the changes in the epigenomic landscape we identified in asthma is/are. As there was minimal overlap between DEX-induced GR binding sites and asthma DERs (Figure S1C), we believe changes identified are not likely the result of current asthma therapies. We observed that many enzymes functioning as writers, readers and erasers of epigenome modifications exhibited differential H3K27ac and gene expression in asthma (Figure S4C and S5B-C). Indeed, enzymes associated with depositing histone modifications themselves were more likely to gain H3K27ac in asthma. However, it is unclear whether these or other asthma-associated changes across the epigenome are cause or consequence. Future longitudinal studies involving larger samples numbers and covering the spectrum of asthma severities are needed to determine when the epigenome is altered in asthma and whether or not there are key 'epigenomic windows' of disease development that might benefit through therapeutic intervention.

Materials and methods:

Ethics and Consent:

This study was approved by the London Bridge Research Ethics Committee (reference 10/LO/1278) and was carried out in accordance with the Declaration of Helsinki and Good Clinical Practice guidelines. Informed consent was obtained from all subjects prior to their participation.

Patient Recruitment:

Volunteers with and without asthma were recruited as previously described(49). None were smokers or had had asthma exacerbations or any respiratory tract infections in the preceding 6 weeks. Asthma was defined as a physician's diagnosis of asthma, and volunteers with asthma had airway hyperresponsiveness (provocative concentration (PC_{20}) of histamine required to reduce FEV_1 by $\geq$20% of $\leq$8 µg/mL, an Asthma Control Questionnaire(50) score >0.75 and were on treatment with inhaled corticosteroids (ICSs) or a combination inhaler (long-acting β agonist + ICS). Healthy controls had a PC_{20} histamine >8 µg/mL. All volunteers with asthma were atopic and all healthy controls non-atopic as determined by skin prick testing (at least one positive skin prick test to a panel of 10 aeroallergens, including grass).

Primary bronchial epithelial cell (BEC) culture:

Bronchial brushings were obtained from volunteers by fibre-optic bronchoscopy using a Keymed BF260 bronchoscope (Olympus, Essex, UK) and 5 mm sheathed endobronchial brushes (Olympus BC-202D-5010) in accordance with British Thoracic Society guidelines(51). Freshly brushed BECs were removed from brushes by agitation and seeded into supplemented bronchial epithelial growth medium (BEBM, Lonza) in a T25 flask. Cell culture was performed as described previously(5), and seeded at passage 2 onto 10mm culture dishes (Primaria, Corning) and cultured until 80% confluent.

Chromatin immunoprecipitation:

BECs were treated with hypotonic solution and mild detergent followed by clarification through sucrose gradients to isolate nuclei. Viability of nuclei was assessed via trypan blue staining. Nuclei were treated with micrococcal nuclease (10U) for 10 minutes at 37°C, re pelleted and supernatant containing mononucleosomes stored at 4°C. Mononucleosomal fractions were incubated with 4µg of H3K27ac antibody (Abcam, Ab4729) and 25µL Protein G dynabeads (Life Technologies) in modified RIPA buffer over night at 4°C. Bound complexes were washed and eluted and ChIP DNA extracted using phenol:chloroform/ethanol precipitation.

Sequencing and analysis:

Libraries were prepared using half total volume of eluted ChIP DNA and NEBNext® DNA Library Prep Master Mix Set and Multiplex Oligos for Illumina® (New England Biolabs). Library quality was assessed using Bioanalyzer 2100 High Sensitivity DNA Gels (Agilent). Libraries were subject to 50bp single end read sequencing on the HighSeq 2500 (Illumina) in rapid run format and reads were aligned to Human genome hg19 using Bowtie2 (Galaxy v2.2.6(52), Table 6). ENCODE and BEC-associated blacklist regions (including chr*N*, chr*Un* and chrM) were subtracted from each BAM file prior to downstream analysis using the *intersect -v* function in bedtools. Sequence reads coverage of BAM files across genome-wide 500kb and 10kb bins was determined using *multiBamSummary* in deepTools (Galaxy v2.1.0)(53) and outputs used in principal component (PAST v3.10(54)) and correlation analyses (*-plot Correlation*, deepTools) respectively. For visualization, Healthy (n=3) and Asthma (n=4) BAM files were merged using samtools (Galaxy), Input BAMs subtracted (-bamCompare) and BigWig's generated and normalized to reads per kilobase per million mapped reads (RPKM, *-bamCoverage*, deepTools).

Differential enrichment analysis:

Differentially enriched regions (DERs) between Asthma (n=4) and Healthy BECs (n=3) were identified across non-overlapping and consecutive 1kb windows genome-wide using MEDIPS v1.20.1(55) (*BSgenome=BSgenome.Hsapiens.UCSC.hg19, uniq=1,*

extend=120, shift =0, window_size=1000, p.adj=bonferroni, diff.method=edgeR, minRowSum=40, MeDIP=F, quantile=TRUE). Significance of DERs genome-wide was visualized with manhattan plots generated using qqman and genomic distribution of DERs determined using CEAS (CISTROME v1.0.0). DERs were annotated using *ROSE_geneMapper.py* (see below) and DER-associated genes identified by ranking all 'closest gene' by number of Gain or Loss DERs and selecting those exhibiting >n=3 DERs/gene (n=3,800 and Figure S1D).

Peak calling and identification of enhancers:

Peaks were called for merged Healthy, Asthma and individual volunteer BAM files using MACS2 (p<5e-4, Galaxy v2.1, Table 6). Typical and Super enhancers (SEs) as defined by Hnisz *et al*.(15) were identified and annotated using Rank Ordering of Super Enhancers algorithm (*ROSE_main.py*, *-t 2000* and *ROSE_geneMapper.py*, *searchwindow=default* respectively)(15). Individual volunteer SEs were compared using *merge -o distinct, count* function in bedtools to identify SE categories. Briefly, to strike a balance between small volunteer numbers and disease heterogeneity, Common SEs were defined as those being present in n=4/7 volunteers, Healthy SEs; n=2/3 healthy volunteers and Asthma SEs; n=3/4 asthma volunteers and no further overlap with any other SE category. dbSUPER(17) overlap analysis (default settings) was used to determine similarity of BEC-SEs with other cell type-SEs and heatmaps were produced using Morpheus (http://software.broadinstitute.org). BEC-SEs were intersected with Asthma DERs and coverage of DERs across BEC-SEs determined using the *intersect* and *coverageBed* options in bedtools. BEC-SE 'metagene' H3K27ac plots were generated using *plotProfile* in deepTools.

Transcription factor motif enrichment:

We refined our genome-wide data further by identifying and focusing on H3K27ac peaks (MACS2) overlapping asthma DERs in motif analysis. Peaks from all volunteer BAMs were merged (n=81,777 total) and intersected with Gain (n=17,083) and Loss DERs (n=11,337) and BEC-SEs (n=12,457). Motif enrichment analysis was conducted using HOMER (*findMotifsGenome.pl -mknown=HOCOMOCOv10 HUMAN mono homer format 0.001.motif* and options for DERs (*-size 150, -h -bg=all DERs*) and BEC-

SEs (*-size 500*)(56, 57). We then selected enriched TFs (P<1e-10) associated with epithelial processes via Ingenuity® (see below) and/or had motifs enriched in BEC-SEs and/or had protein expressed in the respiratory epithelium for further analysis (n=253, see Figure S2A-C). Protein expression and tissue specificity of TFs was determined via Human Protein Atlas (normal tissue data v.16.1)(26). Heatmaps were produced using Morpheus. Peaks in DERs were intersected with published TF sites identified via ChIP-Seq (www.chip-atlas.org) or those predicted using HOMER *annotatePeaks.pl -m=HOCOMOCOv10 HUMAN mono homer format 0.001.motif*. H3K37ac enrichment profiles ±1kb around intersecting peak center were plotted using *plotProfile* in deepTools.

Pathway analysis:

All pathway and biological process enrichment analyses and SE-associated gene categorizations were conducted using Ingenuity® Pathway Analysis Software (QIAGEN).

DNA methylation and epigenomic factors:

Differentially methylated CpGs identified in asthma BECs by Nicodemus-Johnson *et al*.(13) were intersected with DERs and BEC-SEs using bedtools. Overlapping CpGs were further classified by 450K array annotations category ('UCSC_RefGene_Group', Enhancer=True and CpG Island=True). Percentage of CpG content for asthma DERs was determined using HOMER and overlap with ENCODE CpG islands conducted with bedtools. Correlation analysis was conducted using GraphPad Prism v.6. DER-associated genes were classified as epigenomics factors based on Epifactors database(58).

SNPs and chromosomal interactions:

DERs were intersected with Asthma SNPs compiled by Seumois *et al*.(10) or other disease-associated SNPs retrieved from GWAS Integrator. Relationship between SNPs and distance to features of interest was determined using *closestbed -d ref* function in bedtools and binning distances using the *frequency* option in GraphPad Prism v.6. To investigate relationships between long-range interactions, asthma SNPs

and DERs, chromosomal interaction data (Hi-C) was accessed via 3D Interaction Viewer and Database(36). Since no chromosomal interaction data is available for normal airway epithelial cells, we accessed datasets from whole lung tissue and cell types representing components of the respiratory system; fetal lung fibroblasts (IMR90 control,) and epithelium adenocarcinoma (A549). Search parameters were; *Bait*=GSDMA SNPs overlapping DERs (Table S4) and *CLCA1* TSS, *Interaction range=500kb*, *TAD=TopDom (w=20)*. Interactions (5kb resolution) were intersected with asthma SNPs/DERs using bedtools and distance-normalized interaction frequencies of overlapping 5kb bins used to determine strength of SNPs/DER-containing interactions compared all non-DER interactions across the same locus.

Transcriptomics:

We investigated gene expression using published microarray dataset GSE63142(27), the largest study to date of bronchial brushings from healthy controls and mild/moderate and severe asthmatics. Since our ChIP-Seq dataset was derived from mild asthmatics, we focused on mild/moderate asthmatics (n=72) and controls (n=27) and undertook differential gene expression analysis using Partek Genomics Suite (v6.4). After correction for batch effects, ANOVA analysis identified n=4,669 differentially expressed (DE) genes (6,080 probes, $P<0.05$). Relationships between differential gene expression and asthma DERs were determined using BETA (Cistrome v1.0.0, *geneID=Refseq, genome=hg19, peaks=30,000, TSS distance=50,000, CTCF=True, significance=0.05*)(59). Briefly, by assigning a rank number based on the distance between asthma DERs and DE genes (x axis) and plotting them versus the proportion of genes with ranks at or better than the x axis value (y axis), BETA identifies the potential activating/repressing function of asthma DERs on gene expression. The significance of asthma DERs being associated with either up or down regulated genes (above those with no change) is then determined using a Kolmogorov-Smirnov test. In addition, each gene is assigned a rank product (interpreted as a P value) that can be used to identify which differentially expressed genes are mostly likely influenced by asthma DERs (i.e. lower rank product). To be consistent with previous analysis, we selected differentially expressed genes that had >n=3 DERs/gene and identified n=1,592 genes that were potentially influenced

by H3K27ac in Asthma. To further clarify potential activating or repressing function of H3K27ac, expression fold change of each gene was plotted against the negative log_{10} or log_{10} of its rank product if a gene was up regulated (n=779) or down regulated (n=813) respectively.

Targeting acetylation to asthma DERs:

Plasmids encoding active and mutant forms of a deactivated-Cas9-histone acetyltransferase P300 fusion protein (pcDNA-dCas9-p300 Core, pcDNA-dCas9-p300 Core-D1399Y) and guide RNA only expression vector (phU6-gRNA) were gifts from Charles Gersbach(22)(Addgene #61357, #61358 and #53188 respectively). DER-specific gRNAs were designed by submitting DER coordinates or sequence to the CRISPOR (http://crispor.tefor.net) and Breaking-Cas(60) servers respectively and selected based on overlap with BEC DNAse hypersensitivity sites (ENCODE). Control gRNAs to IL1RN were described previously(61). gRNAs were annealed and cloned into phU6-gRNA via *Bbs*I restriction sites (NEB #R0539S). All plasmids were transformed into OneShot®TOP10 competent cells (ThermoScientific), cultured overnight and extracted using Endo Free® Plasmid Maxi or QIAprep® Spin Miniprep (gRNAs) kits (QIAGEN). gRNAs sequence and locations are listed in Table 7.

Cell culture and transfections:

HEK-293T cells were maintained in DMEM media supplemented with 10% fetal calf serum and penicillin/streptomycin at 37°C 5% CO_2. $2x10^5$ cells were reverse transfected with 1µg of dCas9-P300 constructs and 125ng of equimolar pooled or individual gRNAs using Lipofectamine 3000 according to manufacturer's instructions (Thermoscientific). Cells were harvested at 48hrs and RNA extracted (RNAeasy® Mini Kit, QIAGEN). Gene expression was determined via Taqman qPCR assays (Table 7) and run on the Applied Biosystems ViiA™ 7 Real Time PCR system (ThermoFisher Scientific).

Glucocorticoid receptor ChIP-Seq:

FASTQ files from dataset GSE79803(23) was downloaded from SRA (SRP072707) and processed as outlined above. DERs were intersected with dexamethasone- (DEX)-

responsive GR sites as described by Kadiyala *et al*.(23) using bedtools and GR enrichment profiles ±5kb around intersecting sites plotted with deepTools.

Data Accession:

All data has been deposited on gene expression omnibus (GSE109894).

Acknowledgements:

The authors wish to thank Lukas Chavez for advice with differential enrichment analysis (MEDIPS) and Anthony Gerber for glucocorticoid receptor Chip-Seq data.

MRC-GSK Strategic Alliance Consortium list:

Sebastian L Johnston[1,2], Roberto Solari[1,2], Michael R Edwards[1,2], Paul Lavender[2,4], Ross P Walton[1,2], Hannah Gould[2,4], David Cousins[2,4,5], Antoon J. van Oosterhout[3], Jaideep Dhariwal[1,2], Aoife Cameron[1,2], Nathan W Bartlett[1,2], Patrick Mallia[1,2], David J Jackson[1,2,6], Maria-Belen Trujillo-Torralbo[1,2], Jerico del Rosario[1,2], Janet L Smith[3], Matthew J Edwards[3], Karen Affleck[3], Nil Turan Jurdzinski[3], Veronique Birault[3], Peter McErlean[2,4], Yu-Chang Wu[2,4], Nadine Upton[2,4], Ismael Ranz-Jimenez[2,4].

Author affiliations:

[1] Airway Disease Infection Section, National Heart and Lung Institute, Imperial College London, London, UK

[2] MRC and Asthma UK Centre in Allergic Mechanism of Asthma, London, UK

[3] GlaxoSmithKline, Allergic Inflammation Discovery Performance Unit, Respiratory Therapy Area, Stevenage, UK

[4] Department of Respiratory Medicine & Allergy, King's College London, London, UK

[5] NIHR Respiratory Biomedical Research Unit, Department of Infection, Immunity & Inflammation, Leicester Institute for Lung Health, University of Leicester, Leicester, UK

[6] Guy's and St Thomas' NHS Trust, London, UK

Sources of Support:

This work was supported by a Medical Research Council (MRC) and GlaxoSmithKline Strategic Alliance Programme Grant number G1100238, the National Institute of Health Research (NIHR) Biomedical Research Centre funding scheme and the MRC and Asthma UK Centre Grant G1000758. SLJ is the Asthma UK Clinical Chair (grant CH11SJ) and is an NIHR Senior Investigator.

Figure Legends:

Figure 1: Influence of asthma on the epigenome of the airway epithelium.

(A) Correlation analysis of H3K27ac ChIP-Seq data from BECs. The clustering of volunteers into two distinct groups indicates differences in H3K27ac between healthy (blue) and asthma (red) volunteers.

(B) Manhattan plot depicting genome-wide distribution of differentially enriched regions (DERs) of H3K27ac in asthma. Each dot represents an Asthma DER (i.e. 1kb window) plotted in relation to its location and statistical significance. DERs proximal to Th2-high signature genes are highlighted in red. Dashed line represents Adjusted $P<0.05$.

(C) Genome tracks depicting H3K27ac enrichment in BECs across example Gain (*POSTN*) and Loss asthma DERs (*JAK3*). Data tracks from bottom to top; genes (RefSeq annotation), layered H3K27ac from ENCODE, merged data from healthy (n=3, blue) and asthma BECs (n=4, red) and Asthma DERs (black boxes).

(D) H3K27ac enrichment in reads per kilobase per million mapped reads (RPKM) for DERs indicated by arrows in C across all healthy (blue) and asthma volunteers (red; ***$P<0.001$, MEDIPS).

(E) DER-associated genes are enriched in pathways associated with epithelial biology and asthma pathophysiology ($-\log_{10} P$ values, black bars). Pathway analysis also revealed over 25% of genes within the same pathway exhibited differential H3K27ac in asthma (% of pathway genes with DERs, white bars).

(F,G). Examples depicting how numerous components of the same pathway exhibit similar direction of H3K27ac in asthma. The Oncostatin M receptor (OSMR, F) and leukotriene (LT) synthesis pathways (G) predominately gain (red) and lose (blue) H3K27ac respectively. Components in white are unchanged. Genome tracks and dot plots depict H3K27ac enrichment across *OSMR*, *LTC4S* and other pathway-associated genes. Note the transcriptional start site (TSS) of *RICTOR* did not exhibit differential H3K27ac in asthma (star in F genome track). Dot plots represent average enrichment and significance of total DERs/gene indicated below (*$P<0.05$, **$P<0.01$, MEDIPS). Asthma=red, healthy=blue.

Figure 2: Identification of cell-specific and asthma-associated super enhancers in the airway epithelium.

(A) Ranking of H3K27ac ChIP-Seq signal from merged Healthy (blue, n=3) and asthma BECs (red, n=4) identified super enhancers in BECs (BEC-SEs) and associated genes. BEC-SEs were shared (e.g. *KRT80*) and unique to healthy (e.g. *CALML3*) or asthma (e.g. *RAD51B*).

(B) Comparative analysis of SEs from individual volunteers identified three categories of BEC-SEs; those common across all volunteers (airway cell-specific) and those associated with healthy or asthma BECs (see methods and Table 3).

(C) Genome tracks depicting H3K27ac enrichment and presence of asthma DERs across Common (*KRT80* - green), Healthy- (*MUC2* - blue) and Asthma-associated SEs (*MIR31HG* - red). Note no change in H3K27ac is evident at *KLHL9* (star).

(D) Plot depicting log fold change (FC) of all asthma DERs located within BEC-SEs. Asthma BECs exhibited marked changes in H3K27ac across airway cell-specific (i.e. common, green) and healthy- (blue) or asthma- (red) SEs (median ±max-min values, ***P<0.001, ANOVA/ Tukeys multiple comparisons).

(E) Consistent with super enhancers in other cells types, BEC-SE-associated genes included transcriptional regulators (blue). However, we also identified substantial numbers of BEC-SE-associated genes encoded enzymes (yellow).

(F) Pathway analysis indicating that BEC-SE-associated enzymes were enriched in various metabolic processes, particularly those associated with lipids.

(G) Lipid-associated processes (bold) and enzymes encompassed by BEC-SEs (colored as in C).

(H,I) Genome tracks and dot plots depicting H3K27ac enrichment in BECs across lipid-associated enzymes (BEC-SEs colored as in C). Dot plots represent average enrichment and significance of total DERs/SEs indicated below. Asthma=red, healthy=blue. (*P<0.05, **P<0.01, MEDIPS).

Figure 3: Identification of airway epithelium-dominant transcription factors (TFs) associated with H3K27ac in asthma.

(A) Enrichment of TF motifs across asthma DERs and BEC-SEs. Examples of the most enriched and prevalent TF families are indicated.

(B) Heat map depicting motif enrichment, protein expression and tissue distribution of TFs enriched in asthma DERs and BEC-SEs. In addition to epithelial processes, TFs representing other biological process such as circadian rhythm and immediate early genes were identified (see Figure S3 for all TFs). While most TFs were expressed across many tissue types, a subset were enriched in DERs and BEC-SEs and expressed almost exclusively in the respiratory epithelium (bottom panel).

(C) Volcano plot depicting differential gene expression in bronchial brushings obtained from healthy controls and people with mild/moderate asthma(27). Examples of differentially expressed genes encoding TFs binding enriched motifs are highlighted along with other asthma-associated genes as comparison (see Figure S4B for all differentially expressed TFs).

(D) Heatmap depicting expression of Epithelial-dominant TFs highlighted in (C) across all healthy control and asthma volunteers.

(E) Genome tracks depicting H3K27ac across loci encoding epithelium-dominant TFs encompassed by BEC-SEs and asthma DERs (BEC-SEs colored as in 2C). Asthma=red, healthy=blue. (see also Figure S3D)

(F) H3K27ac profiles of healthy (blue) and asthma (red) BECs at epithelium-dominant TF binding sites identified via ChIP-Seq or predicted via HOMER (*). Plots represent enrichment ±1kb around binding site center. Proportion of asthma DERs containing epithelium-dominant TF binding sites are indicated below (see also Figure S3D,E)

(G) H3K27ac enrichment and ChIP-Seq-validated and predicted (*) epithelium-dominant TFs binding sites across epithelial, metabolism and cell recruitment-associated genes. *CLDN1* and *CYP1B1* are encompassed by asthma-associated SE's (red).

Figure 4: Relationship between H3K27ac and DNA methylation in the airway epithelium.

(A) Overlap between asthma-associated changes in DNA methylation identified by Nicodemus-Johnson *et. al(13)*, differential H3K27ac (i.e. DERs) and BEC-SEs.

(B) All differentially methylated CpGs and those overlapping DERs and BEC-SEs categorized with respect to Illumina 450K annotations. DERs were more likely to overlap CpGs contained with CpG islands (CGI's). Note CpGs may overlap more than one annotation category. TSS – transcriptional start site, UTR – un-translated region.

(C) Correlation between changes in CpG methylation and H3K27ac enrichment for all CpGs overlapping DERs, DERs with BEC-SEs and those additionally annotated within CGI's (FC – log fold change). Note correlation for BEC-SEs CGI's included shores and shelves.

(D) Asthma DERs exhibited differences CpG content with loss of H3K27ac in asthma more likely to overlap CpG Islands (CGI's, mean ±max-min, **** $P<0.0001$, Wilcoxon test on ranks).

(E) Despite losing H3K27ac in asthma, dynamic changes in CpG methylation are observed at CGI's across the body (methylated) and TSS (unmethylated) of *JAK3*. For clarity, only differentially methylated CpGs are depicted.

(F) Asthma-associated changes in CpG methylation were more likely to occur in Loss DERs and Common and Healthy SEs. BEC-SE-associated genes with the greatest density of differentially methylated CpGs are indicated (* $P<0.05$, **** $P<0.0001$, ANOVA).

(G) H3K27ac and CpG methylation across Common, Healthy and Asthma-associated SEs outlined in F. For clarity, neighboring CpGs are clustered together. Methylation status in asthma same as in E.

Figure 5: Relationship between H3K27ac and asthma susceptibility in the airway epithelium.

(A) Overlap between asthma-associated SNPs and regions of differential H3K27ac identified in asthma BECs (DERs).

(B) Genome tracks and dot plots depicting H3K27ac enrichment of DERs overlapping asthma SNPs (orange lines and arrows, top track) in healthy (blue) and asthma (red) BECs. A common BEC-SE encompassing *IL6R* is highlighted in green (**P*<0.05, ***P*<0.01, ****P*<0.001, MEDIPS).

(C) Graph summarizing the distance between asthma SNPs and genomic features identified in BECs. Over 70% of asthma SNPs are within ±100kb of an asthma DER.

(D) Genome tracks depicting H3K27ac in BECs and long-range chromosomal interactions in lung tissue (top tracks) across the 17q21 locus. Arcs join regions that interact in three-dimensional space as determined by proximity assays (Hi-C). Purple arcs indicate interactions between SNPs overlapping DERs at *GSDMA* (orange lines, see Table S4) and other DER-containing regions across the locus (5kb bins). Grey arcs and boxes indicate all non-DER interactions and TADs (regions that are compartmentalized together) respectively.

(E) Relationship between interaction distance of *GSDMA* SNPs and loss of H3K27ac across the 17q21 locus. Most interactions with DERs occurred ~100kb downstream at a cluster of DERs encompassing *THRA*.

(F) Interaction frequencies between *GSDMA* SNPs/DERs and other DER-containing regions across tissue/cell types representing the respiratory system. Interactions with DERs encompassing *ORMDL3*, *THRA* and *RAPGEFL1* are strongest, especially in lung tissue. Bars represent mean distance-normalized interaction frequencies of *GSDMA* SNPs (see Table S4) with DER-containing regions ±SEM. Dashed line indicates mean of all interactions across the locus, depicted as purple and grey arcs in panel 3D.

Figure 6: Relationship between H3K27ac and gene expression in asthma.

(A) Plots generated by BETA analysis depicting the relationship between DERs and differential gene expression (DE) in asthma. Overall, gain and loss of H3K27ac was associated with transcriptional activation (up regulated genes - red) and repression (down regulated genes - green) in asthma respectively.

(B) By plotting the predicted activating/repressing function of Gain and Loss DERs versus log fold change (FC) in expression, discordance in the relationship between H3K27ac and expression was identified for a number of genes.

(C) Heatmap depicting expression across all healthy and asthma volunteers in the transcriptomic dataset for genes highlighted in panel 6B.

(D) Genome tracks depicting H3K27ac in BECs at select genes to convey relationships between expression and H3K27ac in asthma. *MUC5B* loses H3K27ac and decreases expression whereas discordance is observed across the Vanin (*VNN1-3,* Gain - down regulated) and Trefoil-factor (*TFF1-3*, Loss - up regulated) gene clusters.

(E) Genome tracks depicting H3K27ac in BECs and long-range chromosomal interactions in lung tissue (top track) across the *CLCA1* locus. Although exhibiting minimal H3K27ac in BECs, *CLCA1* interacts with asthma DERs spanning ~200kb (purple arcs) including those near *CLCA3P* and an asthma-SE at *CLCA2* (highlighted in red). Note no change in H3K27ac is evident at *SH3GLB1* (star).

(F) Relationship between interaction distance of *CLCA1* and gain of H3K27ac in asthma. Most interactions occurred with DERs encompassing *CLCA2* and *CLCA3P*.

(G) Interaction frequencies between *CLCA1* and DERs across tissue/cell types representing the respiratory system. Interactions with DERs encompassing *CLCA2* and *CLCA3P* are strongest in lung tissue and epithelium representative A549 cells respectively. Bars represent mean distance-normalized interaction frequencies of *CLCA1* TSS with DER-containing regions (5kb bins) ±SEM. Dashed line indicates mean of all interactions across the locus, depicted as purple and grey arcs in panel 6E.

Figure 7: Recapitulation of the H3K27ac landscape of asthma BECs in human embryonic kidney (HEK293T) cells and its effect on asthma-associated gene expression.

(A) Genome tracks depicting H3K27ac across *SERPINB2, TLR3* and *TSLP* and location of DER-specific gRNAs (top track - orange lines). An asthma-associated SE is located upstream of *SERPINB2* (red). Regions of 'open chromatin' identified in BECs are depicted in the bottom track (DNase hypersensitivity sites - DHS).

(B) Dot plots depicting H3K27ac enrichment of DERs targeted by gRNAs in A across healthy (blue) and asthma volunteers (red; *P<0.05, **P<0.01, ***P<0.001, MEDIPS).

(C) Using a CRISPR-based approach, acetylation (dCas9-P300-Core) was targeted to asthma-DERs using pooled guide RNAs. Increased P300 indicated successful delivery and expression of dCas9 constructs across all gRNA pools. However, *SERPINB2, TLR3* and *TSLP* gene expression were selectively induced in a DER-specific gRNA and acetylation-dependent manner. Non-DER-targeting gRNAs to *IL1RN* were used as control. Core - only P300 constructs transfected (n=3, Mean ±SEM, *** P<0.001, ANOVA/Tukeys multiple comparisons).

Supplementary Figure legends:

Figure S1:

(A) Principal component (PC) analysis of H3K27ac ChIP-Seq data from Healthy (blue) and asthma BECs (red). Separation of volunteers based on asthma status is most evident across PC2.

(B) Distribution of Gain and Loss asthma DERs across genomic features. As H3K27ac is associated with enhancers, most DERs occurred in distal intergenic sites. Distribution of H3K27ac from ENCODE datasets used as reference. TSS – transcriptional start site, UTR – un-translated region.

(C) Overlap between asthma DERs and dexamethasone (DEX)-responsive glucocorticoid receptor (GR) binding sites identified in the BEAS-2B airway epithelial cell line. Profile plots depict GR enrichment ±5kb around GR binding sites overlapping (inside) and non-overlapping DERs (outside).

(D) Ranking of genes by number of Gain or Loss DERs/gene revealed asthma DERs clustered predominately around certain genes. We selected those genes that contained DERs above the approximate mean (i.e. >n=3 DERs/gene) for further analysis (n=3,800). Example DER-associated genes gaining (black) and losing H3K27ac in asthma (grey) are indicated.

(E) Genome tracks depicting H3K27ac in BECs and the high density of gain and loss DERs across the loci of *KLF5* and *SLC6A10P* respectively. Asthma=red, healthy=blue.

Figure S2:

(A) Relationship between SEs identified in airway epithelial cells compared to SEs identified via H3K27ac ChIP-Seq in other cell types(17). BEC-SEs were most closely related to other mucosal/epithelial cell-type SEs (e.g. esophagus, lung, HMEC).

(B) Overlap between all enhancers (typical and super) identified via MACS2/ROSE (see methods) and asthma DERs identified via MEDIPS.

(C) 'Meta gene' plots summarizing H3K27ac enrichment (RPKM) in healthy and asthma BECs across Common, Healthy- and Asthma-associated SEs. The heatmaps below depict enrichment across all BEC-SE identified (n=1,164). The darker color indicates more H3K27ac enrichment. Differences between healthy and asthma BECs are most evident across Asthma-associated SEs (bottom two heatmaps).

(D) Categorization of all enhancer-associated genes via Ingenuity (see methods).
(E) Similar to asthma, other disease-associated SNPs occurred within ±100kb of an asthma DER. These data may indicate that in order to mediate their effects, SNPs must reside within functional regions such as enhancers, demarcated in this study by H3K27ac. Bracketed numbers indicate total SNPs/disease.

Figure S3:
(A) Work flow used to refine motif enrichment analysis and focus on enriched transcription factors (TFs) important in airway epithelial biology and BEC-SEs.
(B) Ingenuity analysis indicating TFs with motif enrichment in asthma DERs and BEC-SEs were associated with various processes in epithelial biology including epithelial to mesenchymal transition (EMT).
(C-D) Genome tracks depicting H3K27ac in BECs across genes encoding enriched TFs. Most TFs across the sub-categories outlined in Figure 3B (C) and Epithelial-dominant TFs (D) exhibited differential H3K27ac in asthma. *BHLHE40* and *IRX2* are encompassed by a common BEC-SE (green).
(E) H3K27ac profiles of healthy and asthma BECs at TF binding sites identified via ChIP-Seq or predicted by HOMER (* and methods). Plots represent enrichment ±1kb around binding site center. Proportion of asthma DERs containing TF binding sites are indicated below. The paucity of ChIP-Seq data for CLOCK and SOX9 impacted profile interpretation.
(C-E) asthma=red, healthy=blue.

Figure S4 (best viewed online):
(A) Heatmap depicting motif enrichment in asthma DERs and BEC-SEs and protein expression and distribution of all TFs identified via workflow outlined in Figure S3A.
(B-C) Expression of all genes encoding TFs binding enriched motifs (B) or epigenomic modifying factors (C) across all healthy control and asthma volunteers (all genes $P<0.05$ Asthma Vs. Control, ANOVA).

Figure S5:

(A) Correlation between asthma-associated changes in CpG methylation and H3K27ac enrichment across 450K annotation features (FC – log fold change).

(B) Plot depicting log fold change (FC) of all asthma DERs located across DER-associated genes categorized by their epigenomic function or association. Numbers of genes are in parentheses (median ±max-min values, ***P*<0.01, ****P*<0.001, ANOVA/ Tukeys multiple comparisons).

(C) Genome tracks depicting differential H3K27ac in asthma BECs across genes encoding enzymes associated with various epigenomic processes. *KDM6B* is encompassed by a Healthy-associated SE (blue).

Figure S6:

(A) *IL1RN* gene expression was induced in a gene-specific gRNA and acetylation-dependent manner. Core - only P300 constructs transfected (n=3, Mean ±SEM, **** *P*<0.0001, ANOVA/Tukeys multiple comparisons).

(B) *SERPINB2*, *TLR3* and *TSLP* gene expression could be induced with single DER-specific gRNAs in an acetylation-dependent manner (n=3, Mean ±SEM).

(C-D) Genome tracks depicting H3K27ac in BECs across the *SERPINB2* (C) and *IFNB1* locus (D). Acetylation (dCas9-P300-Core) was targeted to DERs upstream of *SERPINB2* within an asthma-associated SE and a virus-inducible enhancer(48) upstream (negative strand) of *IFNB1* using pooled gRNAs (yellow boxes top tracks). No induction of gene expression was observed when targeting enhancer elements. Guide RNAs to the TSS of *SERPINB2* (Pool #1) and *IL1RN* used as controls. Core - only P300 constructs transfected (n=3, Mean ±SEM, ** *P*<0.01, ANOVA/Tukeys multiple comparisons).

Table Legends:

Table S1: Clinical characteristics of study volunteers. ACQ – asthma control questionnaire, FEV_1 – forced expiratory volume in one second, PC_{20} - provocative concentration of histamine to cause a 20% decrease in FEV_1. SPT – skin prick test.

Table S2: Differentially enriched regions (DERs) of H3K27ac in Asthma BECs. Table lists all DERs Adjusted $P<0.05$, associated genes and H3K27ac enrichment across all study volunteers in RPKM.

Table S3: Super enhancers of the airway epithelium. Table lists location, associated genes and coverage of asthma DERs for all common, healthy and asthma associated-SEs.

Table S4: Asthma single nucleotide polymorphisms (SNPs) that overlap regions of differential H3K27ac in asthma BECs (DERs).

Table S5: Asthma-associated genes whose expression is influenced by differential H3K27ac in asthma. The table consists of the top 200 up and down regulated genes that are likely influenced by asthma DERs as determine by lowest rank product score (see methods). To covey the discordance between expression and H3K27ac, both up and down regulated genes are included (100 per Gain or Loss DERs each) along with the number, type and distance of nearest asthma DERs from the gene's TSS. * Dynamic i.e. genes contain both gain and loss DERs ±50kb of TSS.

Table S6: Statistics for H3K27ac ChIP-Seq data and analysis.

Table S7: Sequence and location of DER-specific and control guide RNAs.

Reference List

1. WHO. The Global Asthma Report 2014. Auckland, New Zealand: 2014.
2. Wenzel SE. Asthma phenotypes: the evolution from clinical to molecular approaches. Nature medicine. 2012;18(1546-170X (Electronic)):716-25.
3. Lambrecht BN, Hammad H. The airway epithelium in asthma. Nature medicine. 2012;18(5):684-92.
4. Kicic A, Hallstrand TS, Sutanto EN, Stevens PT, Kobor MS, Taplin C, et al. Decreased Fibronectin Production Significantly Contributes to Dysregulated Repair of Asthmatic Epithelium. American Journal of Respiratory and Critical Care Medicine. 2010;181(9):889-98.
5. Edwards MR, Regamey N, Vareille M, Kieninger E, Gupta A, Shoemark A, et al. Impaired innate interferon induction in severe therapy resistant atopic asthmatic children. Mucosal Immunology. 2013;6(4):797-806.
6. Woodruff PG, Boushey HA, Dolganov GM, Barker CS, Yang YH, Donnelly S, et al. Genome-wide profiling identifies epithelial cell genes associated with asthma and with treatment response to corticosteroids. Proceedings of the National Academy of Sciences. 2007;104(40):15858-63.
7. Gordon ED, Simpson LJ, Rios CL, Ringel L, Lachowicz-Scroggins ME, Peters MC, et al. Alternative splicing of interleukin-33 and type 2 inflammation in asthma. Proceedings of the National Academy of Sciences. 2016.
8. Heinz S, Romanoski CE, Benner C, Glass CK. The selection and function of cell type-specific enhancers. Nat Rev Mol Cell Biol. 2015;16(3):144-54.
9. Yang IV, Schwartz DA. Epigenetic mechanisms and the development of asthma. Journal of Allergy and Clinical Immunology. 2012;130(6):1243-55.
10. Seumois G, Chavez L, Gerasimova A, Lienhard M, Omran N, Kalinke L, et al. Epigenomic analysis of primary human T cells reveals enhancers associated with TH2 memory cell differentiation and asthma susceptibility. Nat Immunol. 2014;15(8):777-88.
11. Kidd CDA, Thompson PJ, Barrett L, Baltic S. Histone Modifications and Asthma. The Interface of the Epigenetic and Genetic Landscapes. American Journal of Respiratory Cell and Molecular Biology. 2015;54(1):3-12.

12. Moheimani F, Hsu ACY, Reid AT, Williams T, Kicic A, Stick SM, et al. The genetic and epigenetic landscapes of the epithelium in asthma. Respiratory Research. 2016;17(1):119.

13. Nicodemus-Johnson J, Myers RA, Sakabe NJ, Sobreira DR, Hogarth DK, Naureckas ET, et al. DNA methylation in lung cells is associated with asthma endotypes and genetic risk. JCI Insight. 2016;1(20):e90151.

14. Yang IV, Pedersen BS, Liu AH, O'Connor GT, Pillai D, Kattan M, et al. The nasal methylome and childhood atopic asthma. Journal of Allergy and Clinical Immunology. 2017;139(5):1478-88.

15. Hnisz D, Abraham Brian J, Lee Tong I, Lau A, Saint-André V, Sigova Alla A, et al. Super-Enhancers in the Control of Cell Identity and Disease. Cell. 2013;155(4):934-47.

16. Whyte WA, Orlando David A, Hnisz D, Abraham Brian J, Lin Charles Y, Kagey Michael H, et al. Master Transcription Factors and Mediator Establish Super-Enhancers at Key Cell Identity Genes. Cell. 2013;153(2):307-19.

17. Khan A, Zhang X. dbSUPER: a database of super-enhancers in mouse and human genome. Nucleic Acids Research. 2016;44(D1):D164-D71.

18. Lovén J, Hoke Heather A, Lin Charles Y, Lau A, Orlando David A, Vakoc Christopher R, et al. Selective Inhibition of Tumor Oncogenes by Disruption of Super-Enhancers. Cell. 2013;153(2):320-34.

19. Peeters J GC, Vervoort Stephin J, Tan Sander C, Mijnheer G, de Roock S, Vastert Sebastiaan J, et al. Inhibition of Super-Enhancer Activity in Autoinflammatory Site-Derived T Cells Reduces Disease-Associated Gene Expression. Cell Reports. 2015;12(12):1986-96.

20. Thakore PI, Black JB, Hilton IB, Gersbach CA. Editing the epigenome: technologies for programmable transcription and epigenetic modulation. Nat Meth. 2016;13(2):127-37.

21. Stepper P, Kungulovski G, Jurkowska RZ, Chandra T, Krueger F, Reinhardt R, et al. Efficient targeted DNA methylation with chimeric dCas9–Dnmt3a–Dnmt3L methyltransferase. Nucleic Acids Research. 2017;45(4):1703-13.

22. Hilton IB, D'Ippolito AM, Vockley CM, Thakore PI, Crawford GE, Reddy TE, et al. Epigenome editing by a CRISPR-Cas9-based acetyltransferase activates genes from promoters and enhancers. Nat Biotech. 2015;33(5):510-7.

23. Kadiyala V, Sasse SK, Altonsy MO, Berman R, Chu HW, Phang TL, et al. Cistrome-based Cooperation Between Airway Epithelial Glucocorticoid Receptor and NF- κ B Orchestrates Anti-inflammatory Effects. Journal of Biological Chemistry. 2016.

24. Wan W-YH, Hollins F, Haste L, Woodman L, Hirst RA, Bolton S, et al. NADPH Oxidase-4 Overexpression Is Associated With Epithelial Ciliary Dysfunction in Neutrophilic Asthma. Chest. 2016;149(6):1445-59.

25. Juncadella IJ, Kadl A, Sharma AK, Shim YM, Hochreiter-Hufford A, Borish L, et al. Apoptotic cell clearance by bronchial epithelial cells critically influences airway inflammation. Nature. 2013;493(7433):547-51.

26. Uhlén M, Fagerberg L, Hallström BM, Lindskog C, Oksvold P, Mardinoglu A, et al. Tissue-based map of the human proteome. Science. 2015;347(6220).

27. Modena BD, Tedrow JR, Milosevic J, Bleecker ER, Meyers DA, Wu W, et al. Gene Expression in Relation to Exhaled Nitric Oxide Identifies Novel Asthma Phenotypes with Unique Biomolecular Pathways. American Journal of Respiratory and Critical Care Medicine. 2014;190(12):1363-72.

28. Chen G, Wan H, Luo F, Zhang L, Xu Y, Lewkowich I, et al. Foxa2 Programs Th2 Cell-Mediated Innate Immunity in the Developing Lung. The Journal of Immunology. 2010;184(11):6133.

29. Park S-W, Verhaeghe C, Nguyenvu LT, Barbeau R, Eisley CJ, Nakagami Y, et al. Distinct Roles of FOXA2 and FOXA3 in Allergic Airway Disease and Asthma. American Journal of Respiratory and Critical Care Medicine. 2009;180(7):603-10.

30. Kushwah R, Oliver JR, Wu J, Chang Z, Hu J. Elf3 Regulates Allergic Airway Inflammation by Controlling Dendritic Cell-Driven T Cell Differentiation. The Journal of Immunology. 2011;187(9):4639.

31. Hackett T-L, Warner SM, Stefanowicz D, Shaheen F, Pechkovsky DV, Murray LA, et al. Induction of Epithelial–Mesenchymal Transition in Primary Airway Epithelial

Cells from Patients with Asthma by Transforming Growth Factor- β 1. American Journal of Respiratory and Critical Care Medicine. 2009;180(2):122-33.

32. Warner SMB, Hackett T-L, Shaheen F, Hallstrand TS, Kicic A, Stick SM, et al. Transcription Factor p63 Regulates Key Genes and Wound Repair in Human Airway Epithelial Basal Cells. American Journal of Respiratory Cell and Molecular Biology. 2013;49(6):978-88.

33. Li CW, Shi L, Zhang KK, Li TY, Lin ZB, Lim MK, et al. Role of p63/p73 in epithelial remodeling and their response to steroid treatment in nasal polyposis. Journal of Allergy and Clinical Immunology. 2009;127(3):765-72.e2.

34. Nemajerova A, Kramer D, Siller SS, Herr C, Shomroni O, Pena T, et al. TAp73 is a central transcriptional regulator of airway multiciliogenesis. Genes & Development. 2016;30(11):1300-12.

35. Schmiedel BJ, Seumois G, Samaniego-Castruita D, Cayford J, Schulten V, Chavez L, et al. 17q21 asthma-risk variants switch CTCF binding and regulate IL-2 production by T cells. Nature Communications. 2016;7:13426.

36. Yang D, Jang I, Choi J, Kim M-S, Lee AJ, Kim H, et al. 3DIV: A 3D-genome Interaction Viewer and database. Nucleic Acids Research. 2018;46(D1):D52-D7.

37. Woodruff PG, Modrek B, Choy DF, Jia G, Abbas AR, Ellwanger A, et al. T-helper Type 2–driven Inflammation Defines Major Subphenotypes of Asthma. American Journal of Respiratory and Critical Care Medicine. 2009;180(5):388-95.

38. Moffett HF, Cartwright ANR, Kim H-J, Godec J, Pyrdol J, Aijo T, et al. The microRNA miR-31 inhibits CD8+ T cell function in chronic viral infection. Nat Immunol. 2017;18(7):791-9.

39. Gonem S, Berair R, Singapuri A, Hartley R, Laurencin MFM, Bacher G, et al. Fevipiprant, a prostaglandin D₂ receptor 2 antagonist, in patients with persistent eosinophilic asthma: a single-centre, randomised, double-blind, parallel-group, placebo-controlled trial. The Lancet Respiratory Medicine.4(9):699-707.

40. Malhotra R, Kurian N, Zhou X-H, Jiang F, Monkley S, DeMicco A, et al. Altered regulation and expression of genes by BET family of proteins in COPD patients. PLoS ONE. 2017;12(3):e0173115.

41. Iwafuchi-Doi M, Donahue G, Kakumanu A, Watts Jason A, Mahony S, Pugh BF, et al. The Pioneer Transcription Factor FoxA Maintains an Accessible Nucleosome

Configuration at Enhancers for Tissue-Specific Gene Activation. Molecular Cell.62(1):79-91.

42. Didon L, Zwick RK, Chao IW, Walters MS, Wang R, Hackett NR, et al. RFX3 Modulation of FOXJ1 regulation of cilia genes in the human airway epithelium. Respiratory Research. 2013;14(1):70.

43. Hand LE, Hopwood TW, Dickson SH, Walker AL, Loudon ASI, Ray DW, et al. The circadian clock regulates inflammatory arthritis. The FASEB Journal. 2016;30(11):3759-70.

44. Durrington HJ, Farrow SN, Loudon AS, Ray DW. The circadian clock and asthma. Thorax. 2013;69(1):90.

45. Leaker BR, Malkov VA, Mogg R, Ruddy MK, Nicholson GC, Tan AJ, et al. The nasal mucosal late allergic reaction to grass pollen involves type 2 inflammation (IL-5 and IL-13), the inflammasome (IL-1[beta]), and complement. Mucosal Immunol. 2017;10(2):408-20.

46. Grubert F, Zaugg Judith B, Kasowski M, Ursu O, Spacek Damek V, Martin Alicia R, et al. Genetic Control of Chromatin States in Humans Involves Local and Distal Chromosomal Interactions. Cell. 2015;162(5):1051-65.

47. Cinghu S, Yang P, Kosak JP, Conway AE, Kumar D, Oldfield AJ, et al. Intragenic Enhancers Attenuate Host Gene Expression. Molecular Cell.68(1):104-17.e6.

48. Banerjee AR, Kim YJ, Kim TH. A novel virus-inducible enhancer of the interferon-β gene with tightly linked promoter and enhancer activities. Nucleic Acids Research. 2014;42(20):12537-54.

49. Dhariwal J, Cameron A, Trujillo-Torralbo M-B, Rosario Ad, Bakhsoliani E, Paulsen M, et al. Mucosal Type 2 Innate Lymphoid Cells Are a Key Component of the Allergic Response to Aeroallergens. American Journal of Respiratory and Critical Care Medicine. 2017;195(12):1586-96.

50. Juniper EF, Bousquet J, Abetz L, Bateman ED. Identifying ‘well-controlled’ and ‘not well-controlled’ asthma using the Asthma Control Questionnaire. Respiratory Medicine. 2006;100(4):616-21.

51. British Thoracic Society guidelines on diagnostic flexible bronchoscopy. Thorax. 2001;56(suppl 1):i1.

52. Afgan E, Baker D, van den Beek M, Blankenberg D, Bouvier D, Čech M, et al. The Galaxy platform for accessible, reproducible and collaborative biomedical analyses: 2016 update. Nucleic Acids Research. 2016;44(W1):W3-W10.
53. Ramírez F, Dündar F, Diehl S, Grüning BA, Manke T. deepTools: a flexible platform for exploring deep-sequencing data. Nucleic Acids Research. 2014;42(W1):W187-W91.
54. Hammer O, Harper DAT, Ryan PT. PAST: Paleontological statistics software package for eduction and data analysis. Paleontologica Electronica. 2001;4(1):9.
55. Lienhard M, Grimm C, Morkel M, Herwig R, Chavez L. MEDIPS: genome-wide differential coverage analysis of sequencing data derived from DNA enrichment experiments. Bioinformatics. 2014;30(2):284-6.
56. Heinz S, Benner C, Spann N, Bertolino E, Lin YC, Laslo P, et al. Simple combinations of lineage-determining transcription factors prime cis-regulatory elements required for macrophage and B cell identities. Mol Cell. 2010;38(4):576-89.
57. Kulakovskiy IV, Vorontsov IE, Yevshin IS, Soboleva AV, Kasianov AS, Ashoor H, et al. HOCOMOCO: expansion and enhancement of the collection of transcription factor binding sites models. Nucleic Acids Research. 2016;44(D1):D116-D25.
58. Medvedeva YA, Lennartsson A, Ehsani R, Kulakovskiy IV, Vorontsov IE, Panahandeh P, et al. EpiFactors: a comprehensive database of human epigenetic factors and complexes. Database. 2015;2015.
59. Wang S, Sun H, Ma J, Zang C, Wang C, Wang J, et al. Target analysis by integration of transcriptome and ChIP-seq data with BETA. Nat Protocols. 2013;8(12):2502-15.
60. Oliveros JC, Franch M, Tabas-Madrid D, San-León D, Montoliu L, Cubas P, et al. Breaking-Cas—interactive design of guide RNAs for CRISPR-Cas experiments for ENSEMBL genomes. Nucleic Acids Research. 2016;44(W1):W267-W71.
61. Perez-Pinera P, Kocak DD, Vockley CM, Adler AF, Kabadi AM, Polstein LR, et al. RNA-guided gene activation by CRISPR-Cas9-based transcription factors. Nat Meth. 2013;10(10):973-6.